FACULTY OF SCIENCE AND TECHNOLOGY

MASTER THESIS

Study programme / specialisation:
Marine and Offshore Technology

The spring semester, 2022

Open / ~~Confidential~~

Author:
Kirill Krotov

.....
(signature author)

Course coordinator: Professor Yihan Xing

Supervisor(s):
Professor Yihan Xing, University of Stavanger
Rasmus Juhlin, Subsea 7 Norway AS

Thesis title:
A Methodology for Sizing Subsea Energy Storage Devices for Offshore Wind-Powered Oil and Gas Platforms

Credits (ECTS): 30

Keywords:
HES
ESS
RES
Wind power
Statistics
Weather window analysis

Pages: 50

+ appendix: 29

Stavanger, 15th June 2022
date/year

Acknowledgements

This thesis fulfilment and the achieved results were thanks to my supervisor's continuous support and supervision, Professor Yihan Xing. I felt more confident and gained a better level of self-research, self-development, communication skills, and alternatives exploration while working under Yihan's supervision. For that, I am deeply thankful.

Also, I would like to thank Professor Lin Li, who provided me with a data and theoretical basis for making this work. Furthermore, I would also like to express my gratitude to my external supervisor, Rasmus Juhlin, for backing connected with the industrial and personal issues.

Furthermore, I am thankful for the helpful tips and advice on making the thesis provided by my groupmates: Egor Smirnov, Usman Ahmad, and Christodoulos Tryfonidis.

Finally, and most importantly, I would like to thank my parents, brothers, and grandparents for the continuous support during this study year filled with both ups and downs. With such a supportive relationship, I feel confident throughout my life.

Kirill Krotov
June 2022
Stavanger, Norway

Abstract

This thesis presents a methodology for sizing subsea energy storage devices for offshore wind-powered oil and gas platforms. This study examines the literature on hybrid energy systems (HES) and subsea energy storage systems (ESS). A subsea energy storage system is proposed as an environmentally friendly and economically feasible solution for power backup. It could be integrated into the power grid of a HES consisting of the ESS, renewable and non-renewable energy sources. It requires an appropriate ESS sizing approach. Two methods of subsea energy storage sizing are presented in this thesis. The first method uses the wind speed expected value. The second method relies on the weather window analysis. Both methods aim to estimate the ESS size capable of working within a chosen period in the power grid of a HES consisting of the wind farm and non-renewable energy source. Correspondingly, the sizing results of an ESS comparing both methods are presented in this work. Finally, initial charging of the device, additional power supply from the shore, and recommendations on future work are discussed. As a result, this study is expected to serve as a guide for planned and existing projects regarding sizing subsea energy storage.

Table of Contents

List of Figures

List of Tables

Chapter 1 - Introduction

Traditional offshore field development is always connected with CO_2 and greenhouse gases, taking up 5.8% of worldwide emissions. Air pollution contributes to global warming. From November 1982 to February 2022 global temperature anomaly increased by 0.72 °C (Our World in Data, 2022). For instance, from 2019 to 2020, greenhouse gas emissions from petroleum activities corresponded to about 12.5 million tonnes of carbon dioxide equivalent in Norway. Still, emissions decreased by 3.5% compared to 1990-2020, when the reduction was only by 4.2% (Norwegian Petroleum, 2022; Statistics Norway, 2021). According to DNV and the Federation of Norwegian Industries Energy Transition, Norway's outlook reports that emissions will be reduced by 24% by 2030 and 79% by 2050 compared to 1990 (Eriksen et al., 2021). On the other hand, in February 2020 Norwegian government updated the goal of reducing emissions by at least 50% and towards 55% below 1990 levels by 2030 (Norwegian government, 2019). Such optimistic forecasts are possible due to modern approaches to reducing atmospheric emissions. They provide a sustainable, clean energy supply that meets power demand from offshore facilities. It was described by KonKraft (KonKraft, 2020) (**Figure 1.1**), including the projects connected with electrification (Riboldi et al., 2019), energy efficiency measures (Nguyen et al., 2016), carbon capture and storage (Roussanaly et al., 2019), and design optimization of the platform (Nguyen et al., 2019).

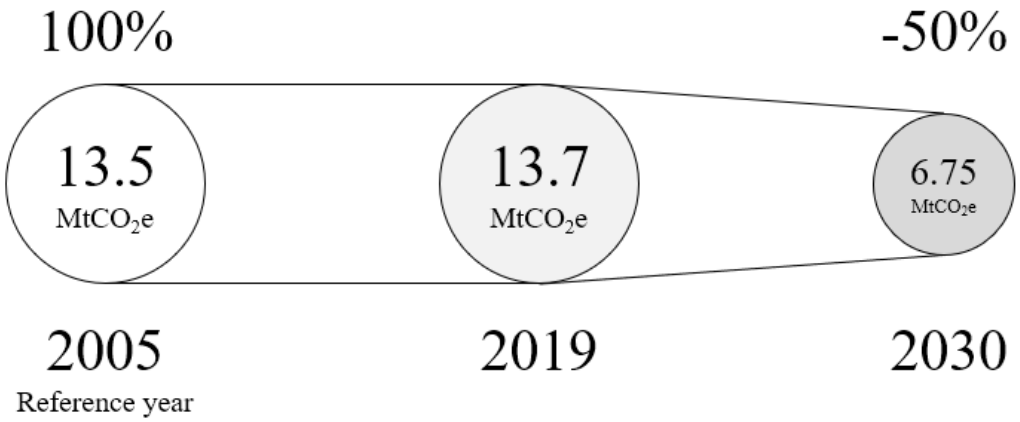

Figure 1.1 Emission reductions from oil and gas production on the NCS by 50 percent in 2030 (Adapted from (KonKraft, 2020)).

A promising approach is the hybrid energy system (HES). It is a concept, which comprises utilizing traditional power generation technologies, such as gas turbines and onshore power sources, in conjunction with renewable energy sources (wind, solar, and hydropower) and

energy storage technologies located on-site, onshore, or subsea. Rafiee and Khalilpour (Rafiee & Khalilpour, 2019) provided an overview of various applications of renewable energy sources in the oil and gas sector. The main focus was on hybridization, highlighting that integrating clean energy sources with the petroleum industry decreases emissions and production costs.

As the leading renewable energy source for HES, wind power is the most developed and promising among other clean energy sources, making significant progress in the oil and gas industry regarding emissions reduction compared to solar and hydropower. Hence, more attention is paid to wind power integration into a power grid system of offshore platforms. There are already investigations of the integration of wind power into simple cycle gas turbines (Aardal et al., 2012; Korpås et al., 2012), the onshore grid (He et al., 2013), and offshore power systems integrated with a wind farm providing optimization and techno-economic assessment (Orlandini et al., 2016; Riboldi & Nord, 2018). However, the viability of proposed strategies is influenced by increased costs of integrating wind power systems into offshore installations (Riboldi et al., 2020) and proper estimation of excess wind power potential. Therefore, adding the energy storage part to the power demand equation could be a helpful solution for handling the irregularity of wind power, the costs of its integration into the hybrid energy system, and utilizing the vast potential of wind excess power.

Integration of the subsea energy storage into the power grid of HES, such as electrolyzers proposed by Riboldi (Riboldi et al., 2020), subsea energy storage by Kloster (Kloster et al., 2021), subsea tanks by Fraunhofer Institute (Hahn et al., 2017) and Massachusetts Institute of Technology (MIT) (Slocum et al., 2013) implies its interconnection with wind energy. Since the wind is intermittent, wind turbines cannot consistently supply power and match the power demand. Wind power output is strongly connected with the wind irregularity, which means that subsea energy storage power contribution is also connected. The subsea energy storage will provide or store power depending on wind power output. Therefore, the subsea energy storage charging will not be constant during the operation period; there will be fluctuations in the charging. Thus, the subsea energy storage system (ESS) must be designed in such a way as to be capable of sustaining these fluctuations in power demand. In other words, it should be appropriately sized.

When it is planned to design HES in conjunction with a wind farm or execute a part of power contribution from the HES (for instance, change the configuration of the gas turbine to a smaller

one) and fill this gap with an energy storage device, a suitable sizing method is required. Since there are several approaches to analyzing the wind data, two methods for ESS sizing are established in this study using 50 years of wind data from the Barents Sea (Reistad et al., 2011). The first method estimates the design ESS size required using the expected wind speed value. The second method estimates the design ESS size using weather windows analysis presented by the cumulative distribution function (CDF) estimation (**Figure 1.2**). This parameter shows the number of weather windows without wind power output due to wind speed exceeding or below the operational boundaries of the wind turbine. Results from this method are then tested through actual historical wind data, where the multiplication factor is empirically fed to adjust the ESS design to the minimum required size capable of operating within the assumed operational period. The aim is to increase understanding of the excess wind power potential and its cooperation with an energy storage device, effectively integrating ESS into a hybrid system by applying the proposed methodology, avoiding unnecessary costs, energy losses, and emissions into the atmosphere.

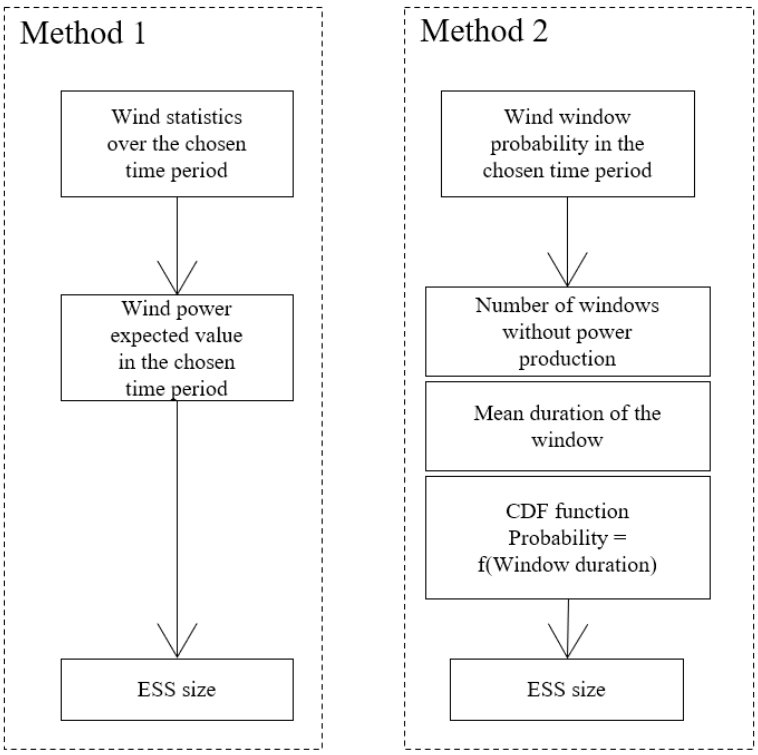

Figure 1.2 Overview of subsea energy storage sizing methods.

According to the background above, the objectives of this thesis work are set in two steps:

(i) Determine the design of HES with subsea energy storage.

(ii) Using the proposed methodology for subsea energy storage sizing for its integration into the power grid of HES and effective utilization of excess power from the wind farm.

This thesis consists of 6 chapters. **Chapter 2** and **Chapter 3** present the literature study of HES and subsea energy storage following this introduction. **Chapter 4** contains the methodology for sizing subsea energy storage with the description of the system used in the sizing and working principles of both sizing methods. **Chapter 5** shows the sizing results of the base case containing a comparison of both methods using such parameters as the accuracy of methods, data sample size, and cut-off (characteristic) value. **Chapter 6** contains discussions and recommendations for future work. Finally, **Chapter 7** summarizes the whole thesis work. In addition, **Appendix A** displays the MATLAB code used to obtain the subsea energy storage sizing results in **Chapter 5**. A paper draft based on the same work has been attached in **Appendix B**.

Chapter 2 – Hybrid energy systems

This chapter will present the literature study of hybrid energy systems (HES). In **Chapter 2.1** main elements, configurations, and possible renewable energy sources (RES) of HES are discussed. Offshore renewable energy sources that could be implemented in the HES are discussed in **Chapter 2.2**.

2.1 Composition and configurations of the hybrid energy system

Wind turbines, solar panels, biomass plants, and hydro turbines are some of the power sources in a hybrid energy system. Excess power is stored in subsea energy storage units, but it may also be configured to draw power from the local electric grid when insufficient reserve power is available.

HES is composed of several components:

- Renewable energy generators (alternating current (AC)/direct current (DC) sources);
- Non-renewable generators (AC/DC sources);
- Power conditioning unit, storage;
- Load (AC/DC) and could include a grid.

The basic structure of the HES is presented in **Figure 2.1**.

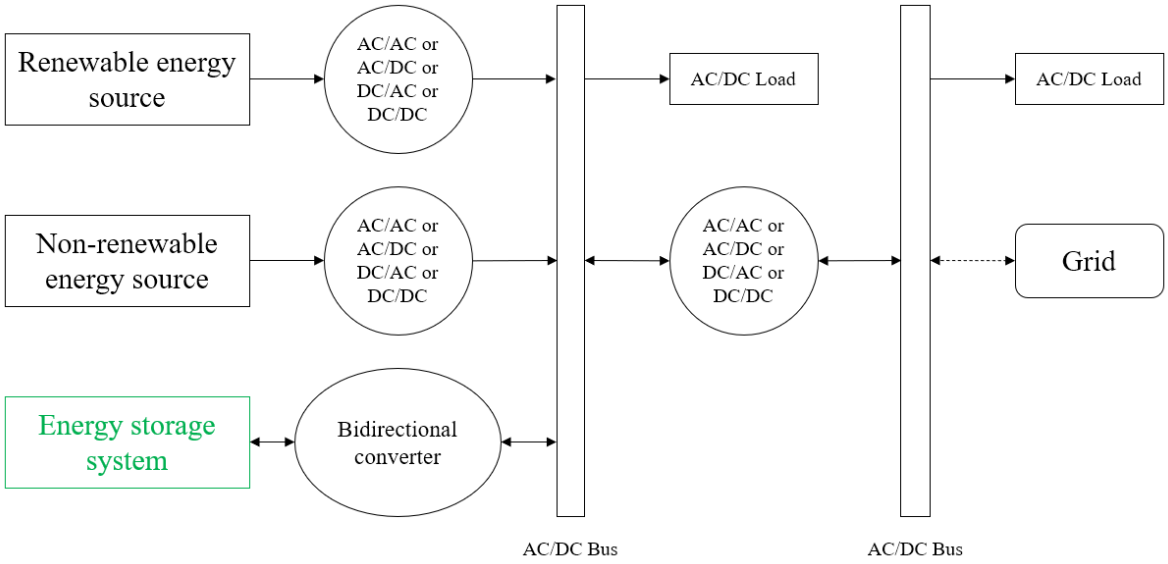

Figure 2.1 Basic structure of the HES.

As be seen, sources and loads could use different types of current (AC or DC). Therefore, HES can be divided according to the transmitting and receiving electricity method. It is presented in **Table 2.1**.

Table 2.1 Configurations of HES.

Configurations	Sources	Loads	Advantages	Disadvantages	Applications
DC-coupled system (Agbossou et al., 2004)	DC	DC	There is no need for synchronization	In this configuration, there is only one inverter, and therefore, if the inverter fails, the system will not be able to meet the load requirements	Low voltage DC microgrid
Power frequency AC coupled system (Maharjan et al., 2008; Rahman & Tam, 1988)	AC	AC	Easier protection	Managing power flow may require coupling indicators	AC microgrid
High-frequency AC coupled system (Cha & Enjeti, 2003)	AC at various frequency	HFAC	The system with high efficiency and reduced size and weight of heat dissipation components	Due to high switching rates, high-frequency power converters suffer high switching losses	Aeroplanes, vessels, submarines, and space station applications
Hybrid coupled system (Nehrir et al., 2011)	AC and DC	AC and DC	Due to the system's flexibility, it can be designed with maximum efficiency and at the lowest cost	Since both AC and DC loads are required for control and energy management, it can be difficult	Power sources and Loads are both AC and DC

Since one of the main components in the power grid of HES is RES, HES could also be divided according to the RES used in the system. For example, it is shown in **Figure 2.2**.

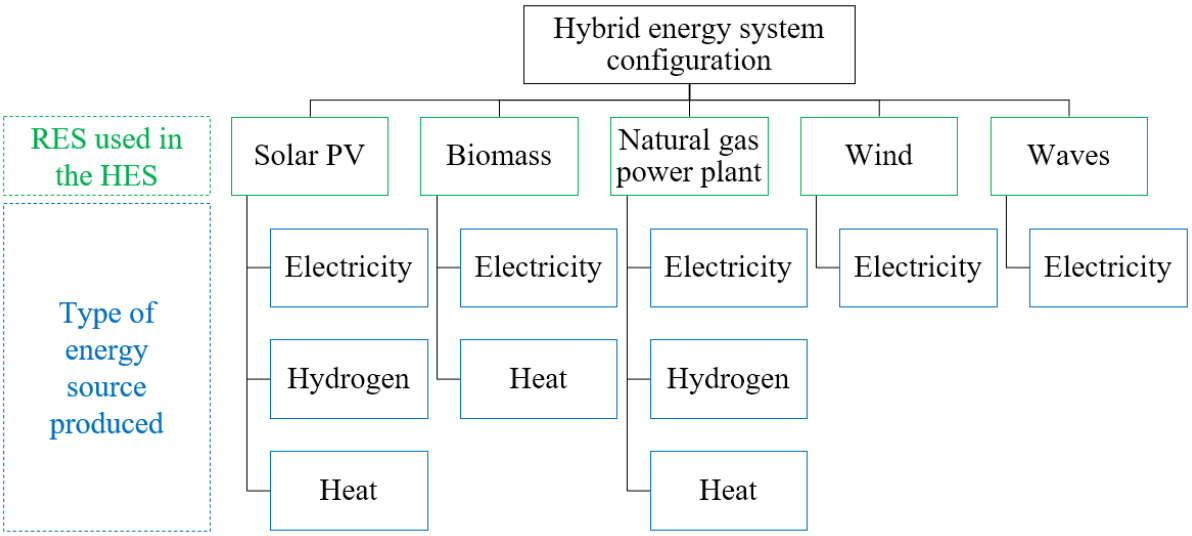

Figure 2.2 HES configuration depending on the used RES.

2.2 Main offshore RES

Since this work focuses on implementing the HES offshore, it is essential to look through the RES, which is applicable offshore.

2.2.1 Solar energy

As the most abundant and easily exploitable natural resource on Earth, solar radiations, also known as electromagnetic radiations emitted by the sun, can generate solar power using solar photovoltaics (PV) and concentrating solar power (CSP) technologies. It is one of the fastest-growing renewable technologies, with a capacity of 481 GW installed in 2018, while CSP technology accounted for around 5 GW (IRENA, 2019; Khan & Arsalan, 2016).

According to Zhang, CSP plants have become increasingly popular due to their high efficiency and low costs (Zhang et al., 2013). Generally, the solar energy plant consists of several components: solar concentrators, receivers, steam turbines, electricity generators, and thermal storage. Using mirrors, solar rays are concentrated and converted into high-temperature heat; this heat is then used to generate electricity through a conventional generator. **Figure 2.3** represents different CSP technologies that could be used with related installed ratios in the technology mix.

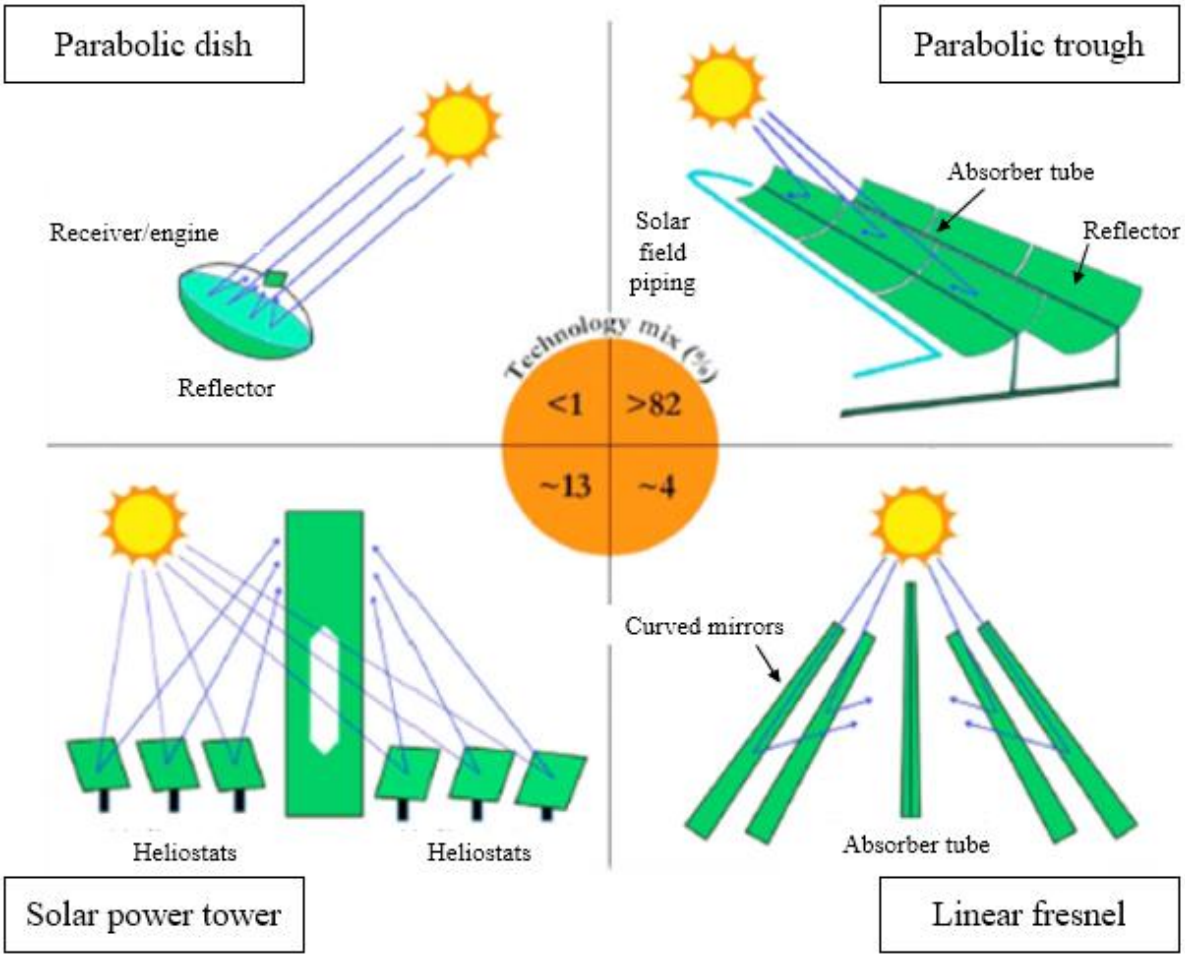

Figure 2.3 CSP technologies classification (Adapted from (Islam et al., 2018)).

On the other side, from the offshore installation perspective, PV arrays were claimed to be more efficient at the commercial stage than CSP (Khan & Arsalan, 2016). It relates to the fact that generating electricity directly from solar rays is possible without using any heat engine by using multiple cells and mechanical and electrical connections in solar PV plants. Furthermore, depending on the material used in the cell (crystalline silicon wafer, thin-film, organic materials), solar cells are divided into three different generations (Husain et al., 2018). PV technologies applicable offshore and their classification is presented in **Figure 2.4**.

Figure 2.4 PV technologies classification (Adapted from (Sahu et al., 2016)).

To sum up, according to investigations by Jibran Khan and Mudassar Arsalan, CSP and PV technologies have pros and cons, and it is not possible which technology is better or worse since it depends on the type of usage and prevailing conditions (Khan & Arsalan, 2016).

2.2.2 Wave and tidal energy

Wave energy is another RES successfully implemented in conjunction with offshore installations. For instance, 21 first-of-a-kind and precommercial marine demonstration projects began production in 2016; 15 were located in European waters; maximum capacities ranged from a few kW to 10 MW. Some are connected to the grid and supply electricity to the grid (Davide et al., 2016).

There is a simple working principle. The ocean waves are created by the wind blowing over the sea surface, caused by the differential heating of the Earth's surface. The technology used for electricity generation from the waves is called wave energy converters (WEC). It captures the kinetic energy of waves and transforms it into electricity. The classification of WEC technologies is presented in **Figure 2.5**.

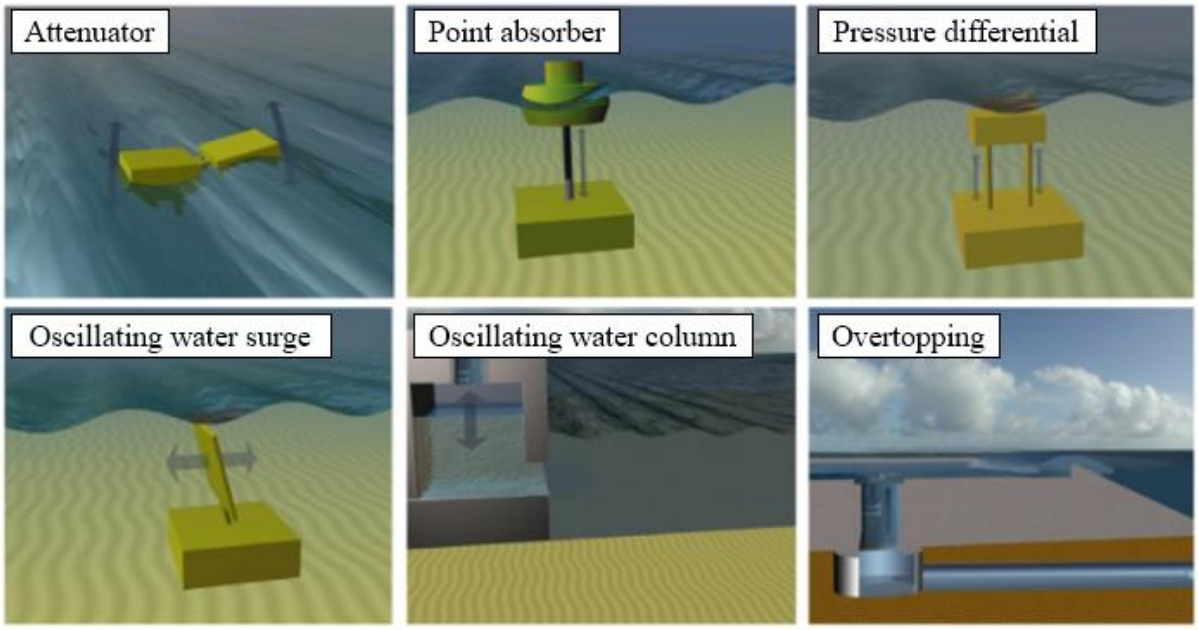

Figure 2.5 WEC technologies classification (Adapted from (EMEC, 2020b)).

Moreover, energy could be produced by the tidal currents or tidal streams caused by the gravitational and rotational forces between Earth, Moon, and Sun (Rourke et al., 2010). Technology for utilizing the energy of flowing water in tidal currents to generate electricity is called tidal energy converters (TEC). The classification of WEC technologies is presented in **Figure 2.6**.

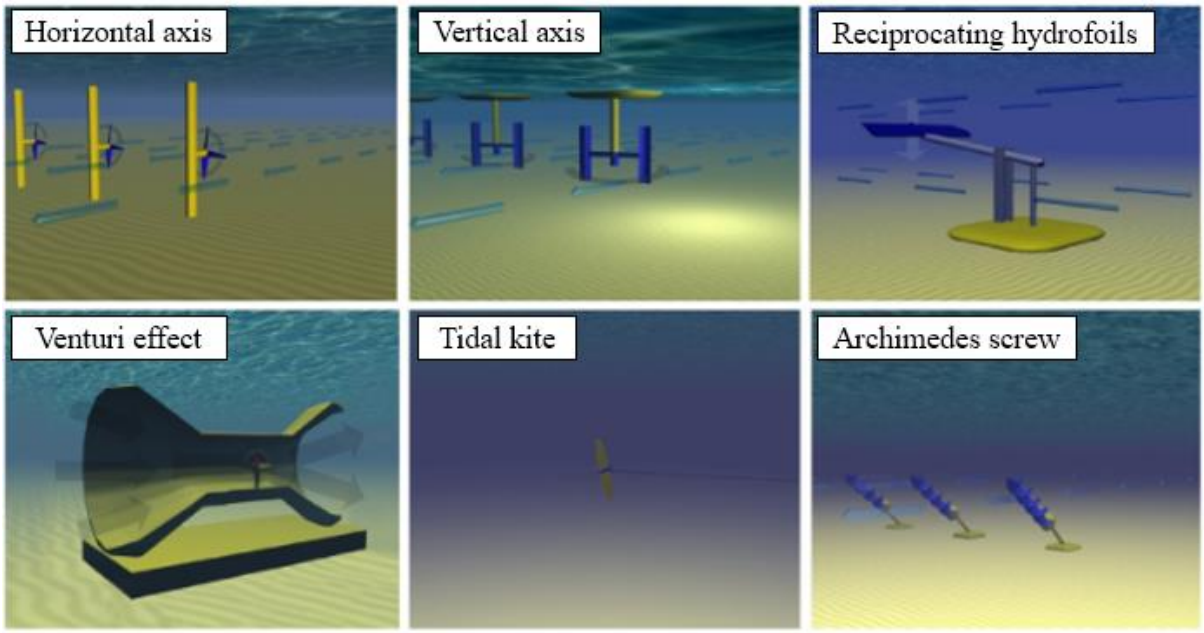

Figure 2.6 TEC technologies classification (Adapted from (EMEC, 2020a)).

Wave energy has reached a commercialization stage, whereas tidal energy has not. On the other hand, in 2014-2016, significant progress was made toward commercialization: 14 tidal energy projects were connected to the grid by the end of 2016 ranging in capacity from a few MW to 14 MW (Davide et al., 2016).

2.2.3 Offshore wind energy

As in **Chapter 1**, the wind is the most promising and commercialized renewable energy source. At the end of 2015, offshore wind power capacity had increased significantly worldwide, reaching 12.1 GW, of which 11 GW were constructed in Europe (Global Wind Energy Council, 2017). A total of 18 GW of offshore wind power capacity was installed in Europe in 2018 because of further growth. The United Kingdom accounted for 44% of all installations in MW, followed by Germany (34%), Denmark (7%), Belgium (6%), and the Netherlands (6%) (Europe, 2018). There are several benefits of an offshore wind RES implementation on the HES:

- high available area to harvest wind energy since there are no limitations relative to urban buildings and human activities;
- stronger and more uniform wind speed with less turbulence;
- limited visual and sound impact.

Wind turbines are a technology used to generate electricity from the wind. The wind itself is produced by uneven heating of the Earth's surface by the sun. Offshore wind energy is electricity generated by the wind in the sea. Due to the increased implementation of this technology worldwide, various offshore wind turbines are presented in **Figure 2.7**.

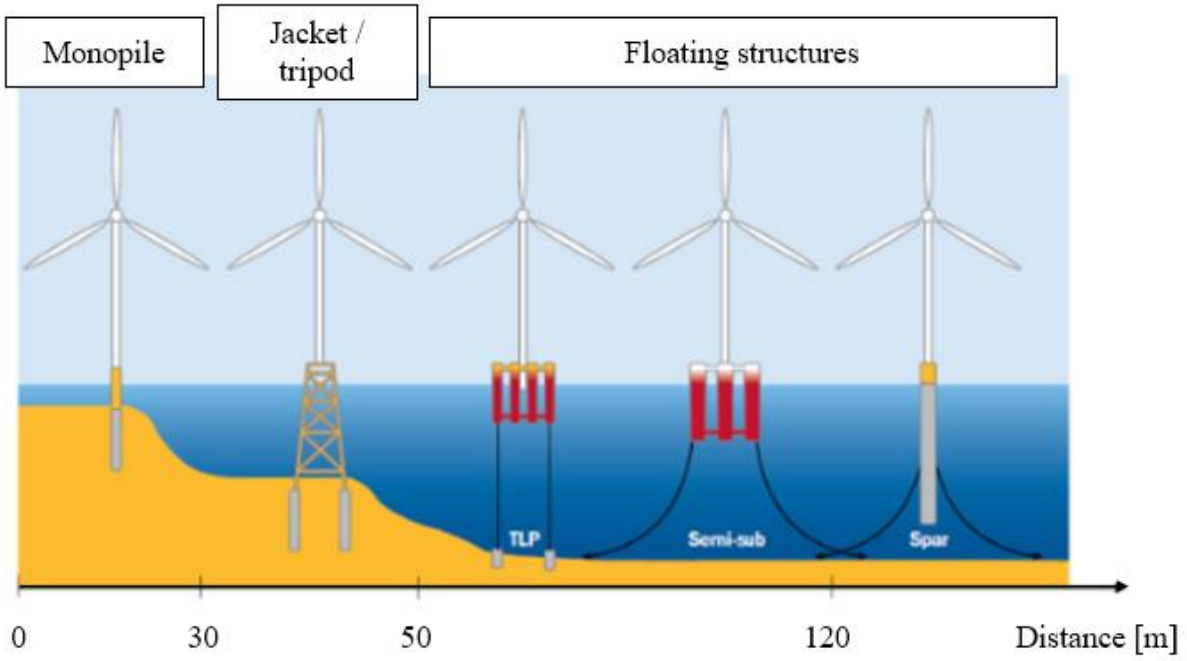

Figure 2.7 Offshore wind turbines classification (Adapted from (Dincer et al., 2021)).

It should be noted that high interest in wind power in this thesis is aroused by the excess wind turbine power potential, which could be used in the HES in conjunction with an energy storage device installed in the power grid of HES. This is described in detail in **Chapter 4**.

2.2.4 Coupling of RES

It is essential to mention that each of the described renewables could be used in conjunction. There are already investigations on large-scale applications of hybrid energy systems with coupled renewable energy sources (Kaldellis et al., 2010; Kapsali & Kaldellis, 2010; Kies et al., 2017; Papaefthymiou & Papathanassiou, 2014). For instance, such an exciting concept was proposed by Jakub Jurasz, where wind- and solar-powered hybrid is integrated into the power system by coupling it with a hydroelectric power station (Jurasz et al., 2018). In **Figure 2.8**, the conceptual design of this system is shown. **Figure 2.9** represents the possible contribution of individual energy sources in covering energy demand.

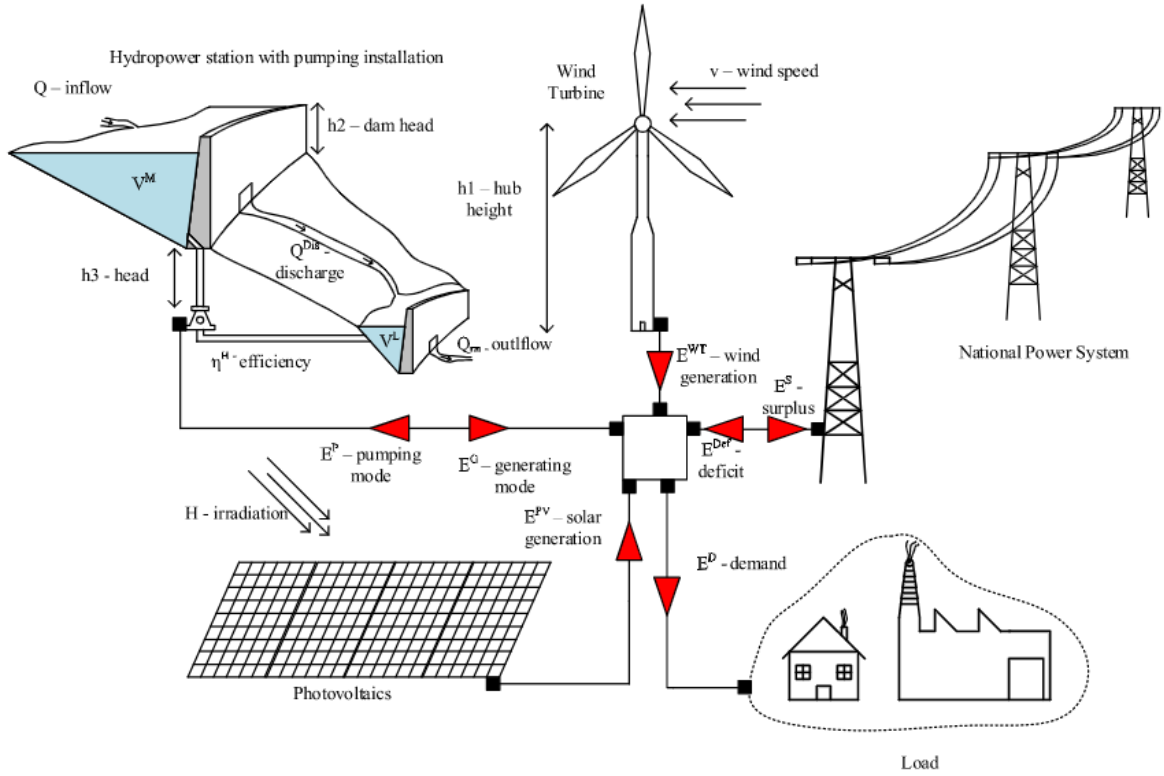

Figure 2.8 Design of the HES with coupled wind, solar and hydro energy sources (Jurasz et al., 2018).

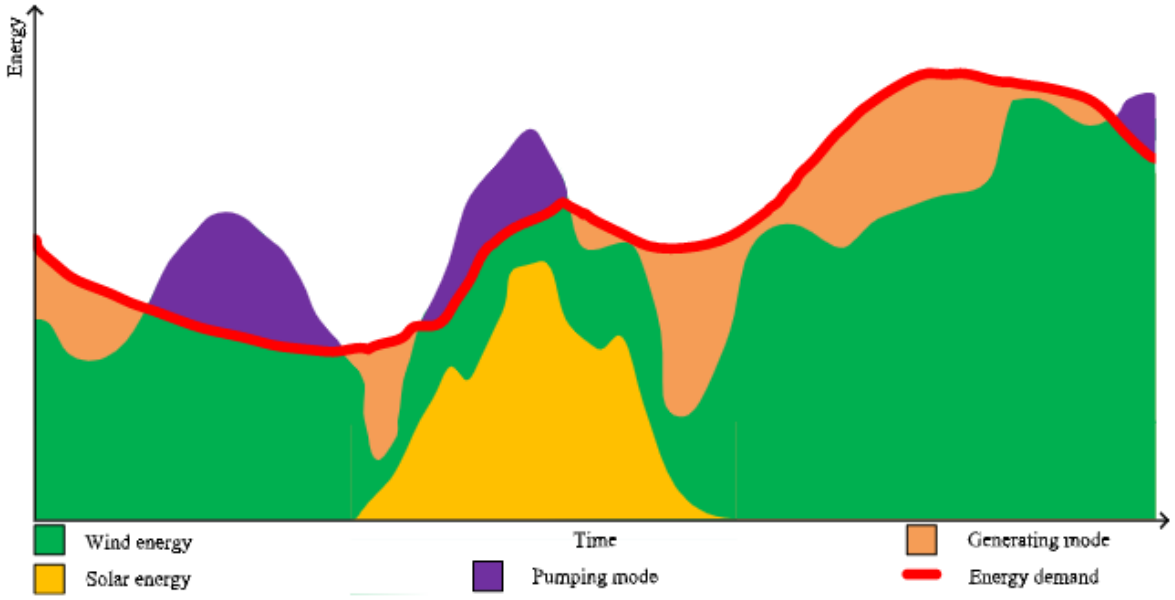

Figure 2.9 Individual energy sources' power contribution (Jurasz et al., 2018).

According to the authors, this concept is universal and can be implemented at any location, especially in locations that must make a trade-off between using water for energy generation. Moreover, using this HES can ease the integration of variable renewable energy sources into the power system.

Chapter 3 – Subsea energy storage systems (ESS)

Hybrid energy system technologies assume the presence of the energy storage part in its power grid. Various energy storage inventions are successfully implemented into the HES available today. In **Chapter 3** literature study on the ESS is conducted, covering most of the subsea energy storage concepts currently being investigated.

Energy storage technologies applicable offshore and combined with RES can be classified as presented in **Table 3.1**.

Table 3.1 Classification of the ESS technologies.

Technology classification	Core technology	Working principle
Mechanical	CAES (Compressed Air Energy Storage) (Budt et al., 2016)	The storage is charged using electrically driven compressors, which convert the electric energy into potential energy, or exergy, of pressurized air. The pressurized air is stored in CAS volumes of any kind and can then be released upon demand to generate electricity again by the expansion of the air through an air turbine
	Flywheels	
Electrochemical	Secondary Battery	Uses two electrodes and two different circulating electrolyte solutions, a positive and a negative, to convert and store electrical energy in the form of chemical energy and then convert that stored energy back into electrical energy
	Flow batteries (Lundin & Beitler-Dorch, 2018)	
Electrical	SMES (Superconductor Magnetic Energy Storage) (Chen et al., 2006)	Stores energy in the magnetic field
	Supercapacitors	
Chemical (Hydrogen)	Power to Power (fuel cells, etc.) (Riboldi et al., 2020)	Hydrogen energy conversion system that converts the stored chemical energy in hydrogen to electrical energy, also producing water and heat as by-products with no carbon emissions
	Power to Gas	
Hydro	Subsea Energy Storage (Kloster et al., 2021)	Generates electricity when water comes in and stores electricity when water is pumped out
	StEnSea (Stored Energy in the Sea) (Hahn et al., 2017)	
	ORES (Ocean Renewable Energy Storage) (Slocum et al., 2013)	
	Ocean Battery (Hut, 2020)	

Overview of the designs of the ESS technologies are presented in **Figure 3.1**

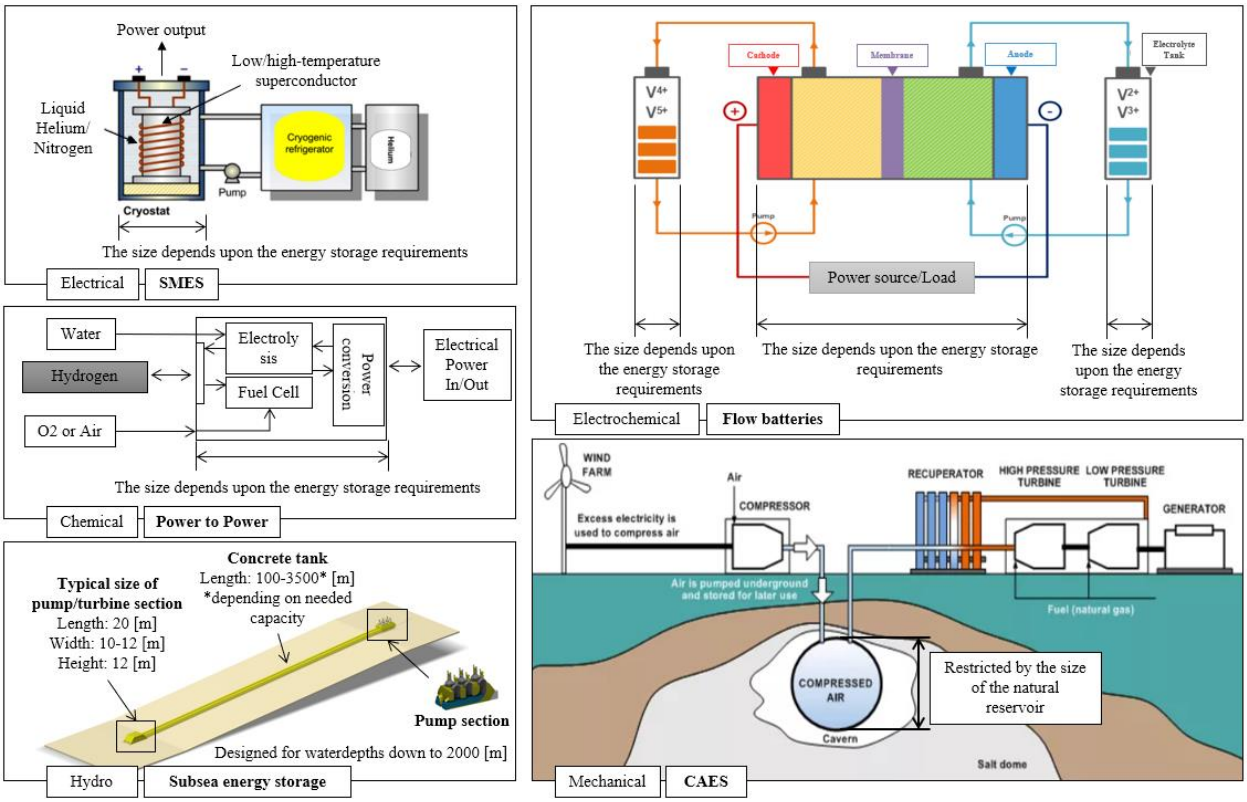

Figure 3.1 Overview of the energy storage designs.

Chapter 4 - Methodology for sizing subsea energy storage devices

Chapter 4 overviews the methods used for sizing the energy storage system. A description of the system used in the proposed methodology is presented in **Chapter 4.1**. Next, both methods analyze the wind data and distribution described in **Chapter 4.2**. Furthermore, an overview of methods 1 and 2 are presented in **Chapter 4.3** and **Chapter 4.4**, respectively. Finally, verification of the methods through 50-years data is shown in **Chapter 4.5**.

4.1 System description

4.1.1 Hybrid energy system

The hybrid energy system for offshore oil and gas platforms combines an energy storage device, gas turbines, an offshore wind farm, and power from shore. Gas turbines (GTs) and onshore power sources are primary power sources. These provide the base-load power to the offshore installations. The offshore wind farm and ESS provide the remaining power. In case of excess power from the wind turbine, it is stored in the ESS and used when needed. Conversely, ESS supplies the required amount of power without wind power. **Figure 4.1** presents a schematic of the HES, where one of the ESS concepts proposed by Ernst Kloster (Kloster et al., 2021) is shown.

There are several options for how power can be supplied to the offshore facility:

1. Gas turbine + Wind farm + ESS
2. Onshore power + Wind farm + ESS
3. Gas turbine + Onshore power + Wind farm + ESS

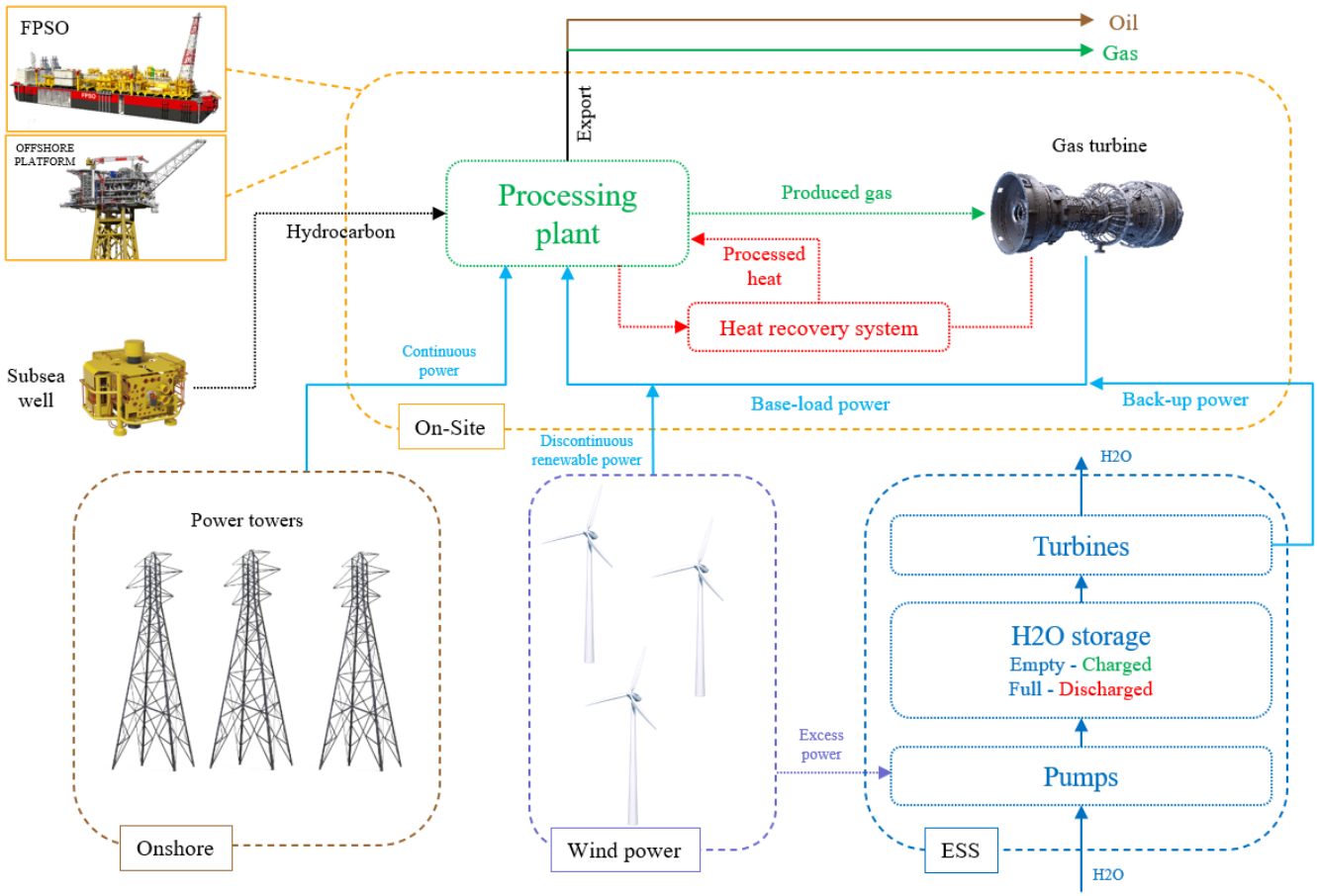

Figure 4.1 Schematic representation of the hybrid energy system using subsea ESS.

This part describes the main power contributors of the hybrid energy system. The following process components meet the power demand of the offshore installation (**Equation 4.1**):

$Load = P_{GT} + P_{WT} + P_{ESS}$	**Equation 4.1**

Where $Load$ is a power demand from the offshore platform, P_{GT} is gas turbine power output, P_{WT} is the wind power output, P_{ESS} is the power output from the ESS. All values are measured in megawatts (MW).

The power demand from the offshore platform and on-site facility is constant throughout the operating period.

Gas turbines GE LM6000 PF with a rated power of 44.7 MW and GE LM2500 + G4 with a rated power of 33.3 MW examined by Riboldi (Riboldi et al., 2020) were chosen as the primary on-site power source. It is an aero-derivative gas turbine, usually used in offshore applications (Riboldi et al., 2019).

4.1.2 Wind power

The NREL offshore 5-MW baseline wind turbine was chosen as the primary source of wind power for this work (Jonkman et al., 2009). The characteristics of the wind turbine are presented in **Table 4.1**. Wind turbine power output depending on the wind speed is presented in **Figure 4.2**.

Table 4.1 Properties of the NREL 5-MW wind turbine.

Parameter	Units	Value
Rating	[MW]	5
Rotor Orientation, Configuration	-	Upwind, 3 Blades
Control	-	Variable Speed, Collective Pitch
Drivetrain	-	High Speed, Multiple-Stage Gearbox
Rotor, Hub Diameter	[m]	126, 3
Hub Height	[m]	90
Cut-In, Rated, Cut-Out Wind Speed	[m/s]	3, 25
Cut-In, Rated Rotor Speed	[rpm]	6.9, 12.1
Rated Tip Speed	[m/s]	80
Overhang, Shaft Tilt, Precone	[m],[º],[º]	5, 5, 2.5
Rotor Mass	[kg]	110,000
Nacelle Mass	[kg]	240,000
Tower Mass	[kg]	347,460

Since proposed approaches for ESS charging estimation rely on the irregularity of wind power, it should be noted that this aspect is strongly connected with the wind and environmental conditions in the operated region.

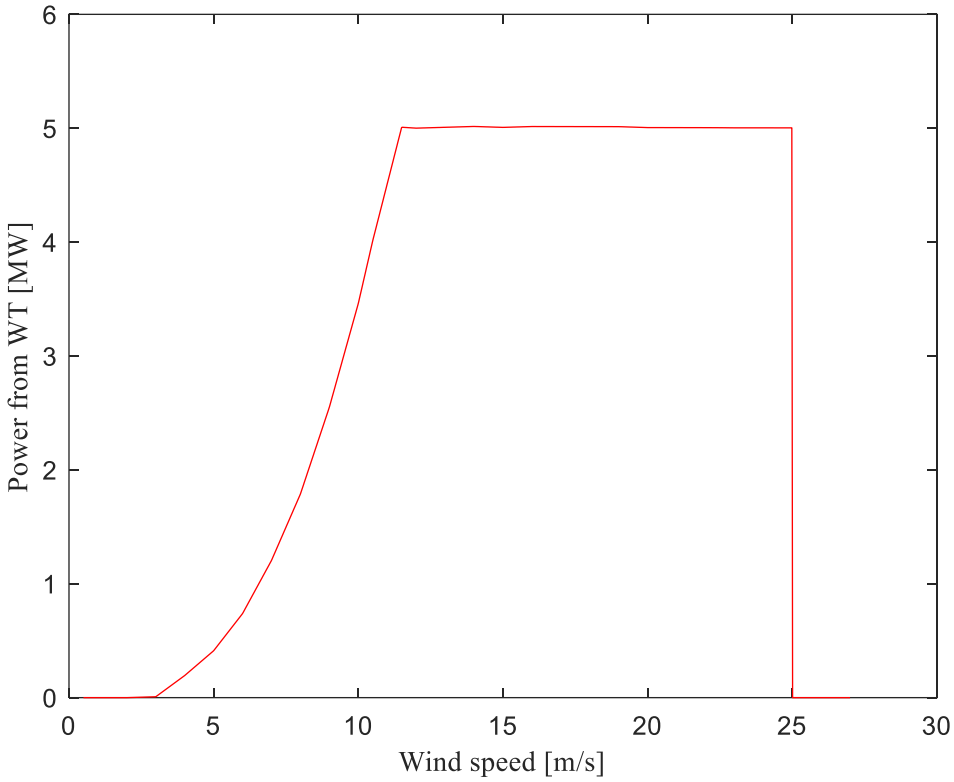

Figure 4.2 Wind turbine NREL 5 MW power output dependence on wind speed.

4.2 Wind distribution

Wind speed distributions can be approximated well by the two-parameter Weibull distribution (Bitner-Gregersen, 2005; Bitner-Gregersen & Haver, 1991), and the probability density function (PDF) is given by **Equation 4.2**.

$f_{U_w}(u) = \frac{\alpha_U}{\beta_U}(\frac{u}{\beta_U})^{\alpha_U - 1} * \exp\left[-(\frac{u}{\beta_U})^{\alpha_U}\right]$	**Equation 4.2**

Where α_U and β_U are the scale and shape parameters, respectively, and u is the wind speed variable, $f()$ refers to the PDF. It is shown in **Figure 4.3**.

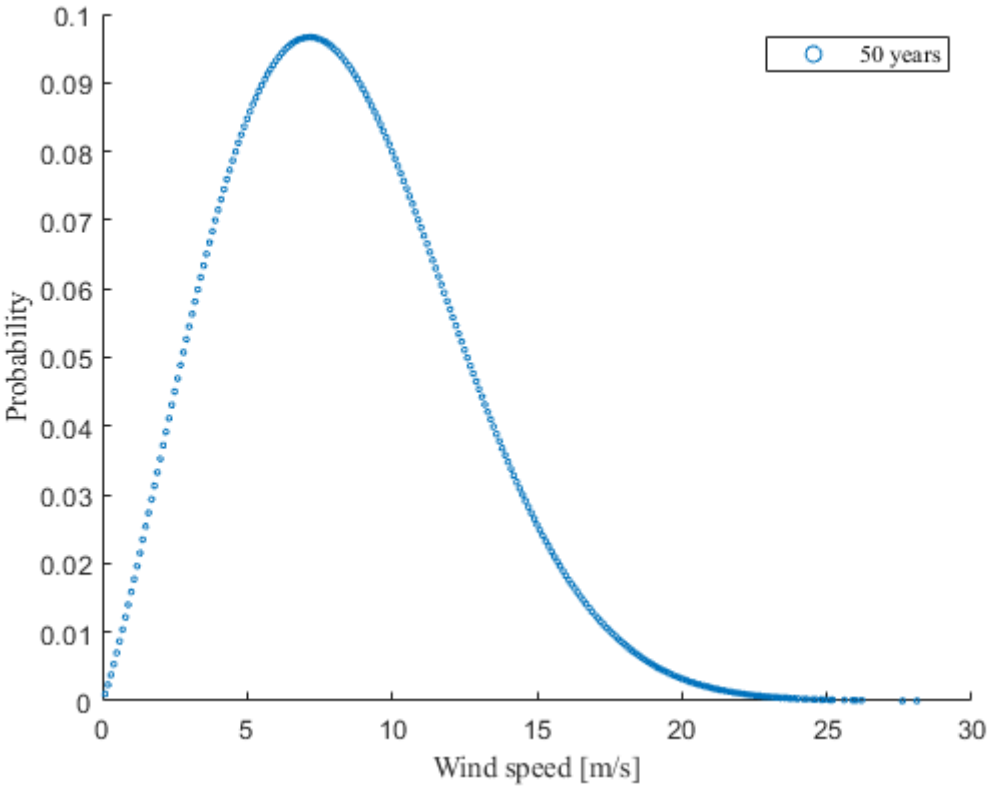

Figure 4.3 Weibull distribution for wind speed 50 years data in the Barents Sea.

Since the data can be measured at different heights scaling parameter is needed to be used, which is represented by the **Equation 4.3** (Li et al., 2015):

$U(z) = U_h * (\frac{z}{h})^{\alpha}$	**Equation 4.3**

Where z represents the height, U_h is the mean wind speed at the reference height h [m], $\alpha = 0.1$ - constant wind speed profile parameter.

4.3 Method 1: ESS sizing using expected wind speeds

This method refers to the sizing of an energy storage device considering wind power's expected value. Since the wind speed varies, there is a different power contribution from the wind turbine at each time point. However, at the same time, a value occurs most often and can be obtained mathematically.

Firstly, the wind speed expected value is needed to be found. Using Weibull distribution from **Equation 4.2**, shape parameter (β_U) and scale parameter (α_U) are obtained. These parameters are used to find the expected wind speed value (**Equation 4.4**).

$\overline{S_{wind}} = \alpha_U \, [\Gamma(1 + {\beta_U}^{-1})]$	**Equation 4.4**

Where $\overline{S_{wind}}$ – wind speed expected value [m/s].

Secondly, using linear interpolation relying on the data from the **Figure 4.2** wind power expected value is calculated (**Equation 4.5**).

$\overline{P_{wind}} = P_{wind_t} + \frac{P_{wind_{t+1}} - P_{wind_t}}{S_{wind_{t+1}} - S_{wind_t}} (\overline{S_{wind}} - S_{wind_t})$	**Equation 4.5**

Where $\overline{P_{wind}}$ – wind power mean (expected) value [MW], t – data point, P_{wind_t} – wind power value in specific data point [MW], S_{wind_t} – wind speed value in specific data point [m/s].

Finally, ESS size is estimated by solving simple **Equation 4.6**.

$\overline{P_{ESS}} = \overline{Load} - \overline{GT} - \overline{P_{wind}}$	**Equation 4.6**

Where $\overline{Load}$ is the mean installed demand from the offshore platform and facility, $\overline{GT}$ is the mean power supply from the gas turbine. All values are measured in MW.

4.4 Method 2: ESS sizing using weather windows

The novelty of this work lies in the fact that weather window analysis is used to size the energy storage. Due to the intermittent wind, there are weather windows where the wind speed value is such that the wind turbine cannot generate power. Therefore, the maximum duration of the window is used to size ESS. Investigations are based on the 50-years wind data in the Barents Sea with 3-hour discretization (Reistad et al., 2011).

Firstly, depending on the type of the wind turbine (different hub heights, where extreme wind speed values are determined), **Equation 4.3** establishes wind speed boundaries, above and lower, of which there is no power production (**Figure 4.4**).

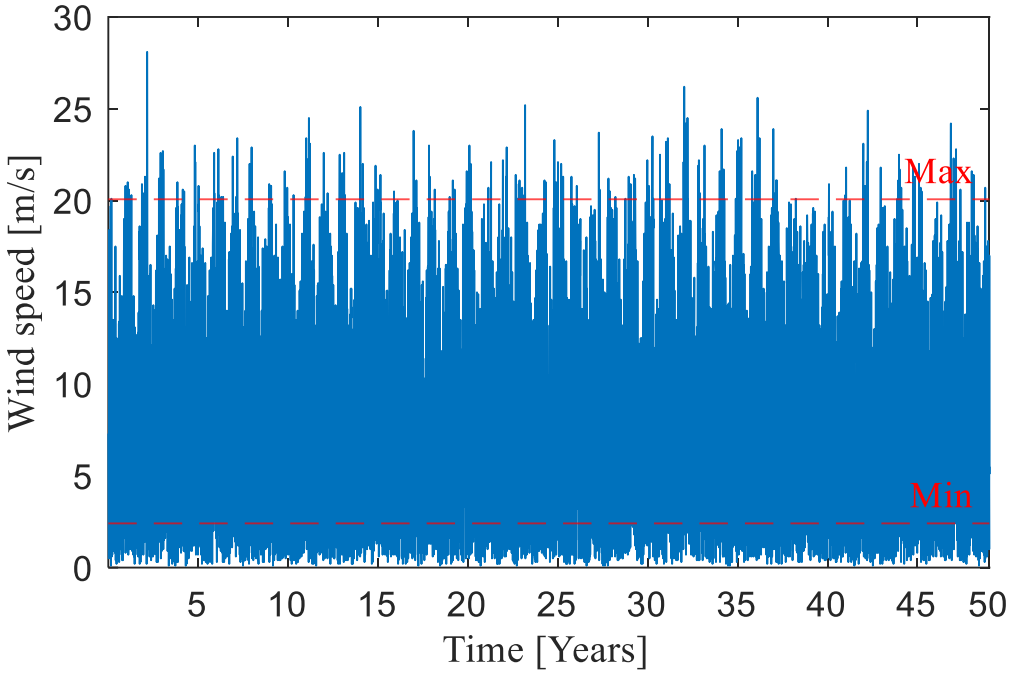

Figure 4.4 Wind speed boundaries within 50 years.

Secondly, suppose a random sample size N (wind speed 50-year data) from a distribution. In that case, we often estimate the cumulative distribution function (CDF) of that distribution by the empirical distribution function, which is just the number of observations divided by the total number N. In other words, the empirical distribution function is the distribution function of the discrete distribution, which puts probability 1/N on each of the observations. Using **Equation 4.7**, empirical CDF of the weather window durations is obtained. It shows that below a particular probability, the particular duration of the window is likely to occur (Li et al., 2021).

$$Empirical\ CDF = \frac{i = 1, \dots, N}{N}$$	**Equation 4.7**

Where i – specific weather window, N – total number of weather windows without wind power output within 50 years.

Finally, according to the chosen cut-off (characteristic) value of the empirical CDF, which is equal to 0 to 1, the value of non-productive hours (weather window duration) for which ESS should be designed is obtained. Then, estimation of the ESS size is done as follows (**Equation 4.8**):

$E_{ESS} = \left(\overline{Load} - \overline{GT}\right) * h(p), p \in [0,1]$	**Equation 4.8**

Where E_{ESS} – ESS charging [MW*h], h - weather window duration (non-productive hours) [h], p – cut-off (characteristic) value of empirical CDF.

4.5 Verification of methods 1 and 2 through 50-years data

At this stage, the multiplication factor is introduced, which is empirically fed to adjust the ESS design obtained in method 1 and method 2 to the minimum required size capable of operating within 50 years. (**Equation 4.9**).

$1\ method: ESS_{50\ years} = \overline{P_{ESS}} * n$ $2\ method: ESS_{50\ years} = E_{ESS} * m$	**Equation 4.9**

Where n - number of hours ESS should be designed to be capable of sustaining 50 years [h], m - multiplication factor.

Chapter 5 – Sizing of the subsea energy storage on the Norwegian continental shelf for offshore wind-powered oil and gas platform

Chapter 5 discusses the results of the ESS sizing using methods 1 and 2. It explains the expected size of the energy storage system (device) in the hybrid energy system (Ref. **Chapter 5.1.1**), the differences between both methods (Ref. **Chapter 5.1.2**), comparing different parameters and relevant multiplication factors (Ref. **Chapter 5.1.3**). Again, methodology and the system discussed in **Chapter 4** are used.

5.1 Base case

The Norwegian continental shelf was chosen as the study area. According to Legorburu (Legorburu et al., 2018), this area is considered extremely promising for combining an offshore petroleum production facility and offshore wind farms when evaluating technical, environmental, and market aspects. There are 15 zones on the Norwegian shelf, including zones considered for bottom-fixed installations and floating turbines with a capacity factor is estimated to be in the range of 36–50% (from 4600 to 12600 MW), with an estimated average production of 19 – 60 TWh (Legorburu et al., 2018). This assessment is supported by He (He et al., 2010), which describes that offshore wind displays higher average wind speed, lower wind shear, and turbulence intensity.

An offshore facility located in the Norwegian sector of the Barents Sea is used as a case study. The input data is presented in **Table 5.1**.

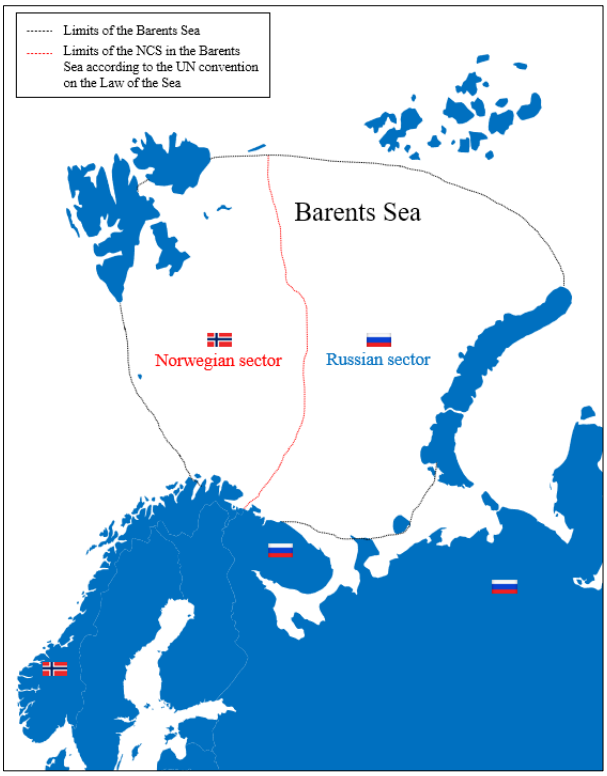

Figure 5.1 Norwegian and Russian sectors of the Barents Sea.

Table 5.1 Input data. Base case.

Parameter	Unit	Value
Load from the offshore platform and facility	MW	45.0
Gas turbine installed power output	MW	44.7
Gas turbine workload	-	0.95
Gas turbine-operated power output	MW	42.5
Number of wind turbines	-	5
The initial state of charge of the ESS	%	50

The following aspects have been investigated:

- Size of the subsea energy storage.
- Comparison of the methods.
- Data samples influence the results.
- Initial charging of the ESS.

5.1.1 Size of the storage required

Results of this work show that a considerable amount of power for ESS is needed to maintain constant power demand from the offshore facility. More than 500 MWh of energy ESS should be capable of storing for 50 years of operation (**Table 5.2**). Method 1 and 2 show comparable results varying from 2 – 10 percent depending on the wind power expected values, CDF curve, and cut-off (characteristic) values used in the analysis.

Table 5.2 Method 1, 2. ESS required charging for 50 years. Base case.

Method	P^{*}_{ESS}, **MWh**
Method 1	510
Method 2	

* - operated years = 50 years, assumed as work-life of an offshore project

Charging of the ESS is not constant during the operation period. There is always a surplus or deficit of power in the hybrid energy system due to wind power irregularity (**Figure 5.2**). The methods proposed in this paper help design ESS size capable of operating within a different assumed time range and wind speed variations.

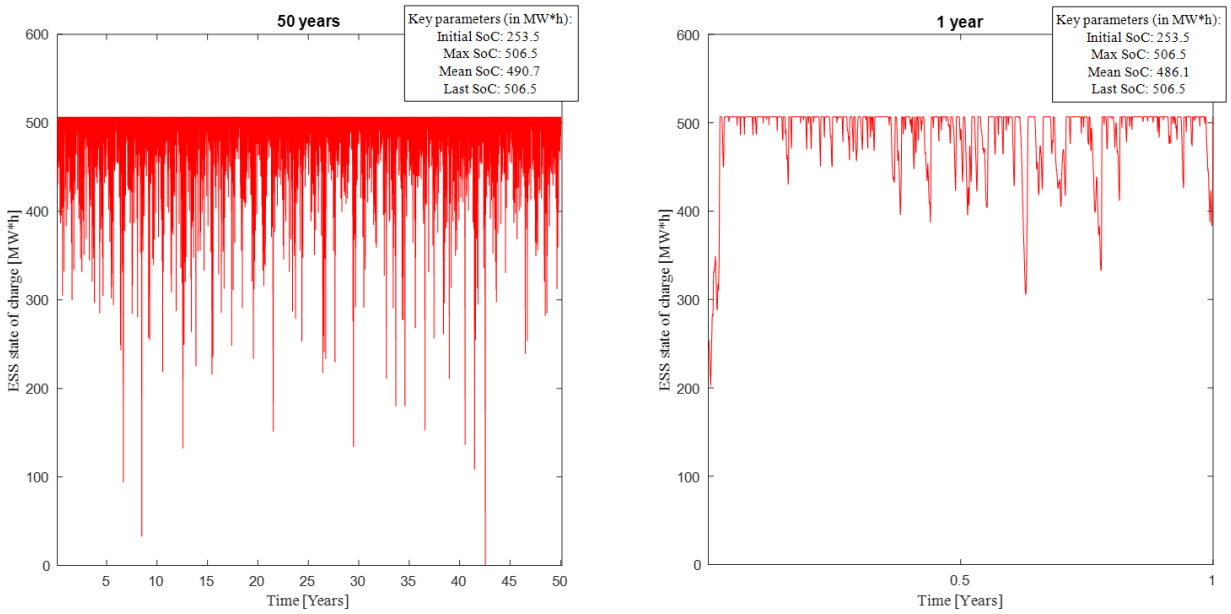

Figure 5.2 Method 1 - ESS state of charge over 50 years (left) and over 1 year (right) using wind power expected value for 50 years and 50 percent of initial charging.

5.1.2 Method 1 vs Method 2

Accuracy of methods

As mentioned in **Chapter 5.1.1**, method 1 and method 2 show comparable results, equal to the 510 MW*h on average. Thus, both methods are applicable for estimating the ESS size and are comparable relative to each other. However, regarding complexity, Method 1 is more intuitive and straightforward to understand than the second method, where weather window analysis is used. Moreover, for Method 1, less wind data is needed, which is well-described in the next section.

Data sample size

Both methods clearly show that a large ESS should be constructed for 50 years of operation. To obtain the values of the size, multiplication factors were used. In Method 1 multiplication factor is equal to the number of hours for which ESS should be designed. In Method 2, this factor shows the value which should be applied to initially calculated ESS charging. It gives a result equal to the ESS size capable of operating within 50 years.

Table 5.3 Method 1. Sizing results. Base case.

Data sample*	$\overline{P_{wind}}$, **MW**	$\overline{P_{ESS}}$, **MW**	$n^{**}_{50\ yrs}$, **hours**
1 year	1.66	0.88	578***
15 years	2.02	0.52	976
25 years	2.03	0.51	998
50 years	2.07	0.46	1090

* - data sample in which wind power expected value is evaluated (return period)

** - mean energy storage capacity is tested in 50-years data

*** - multiplication factor - number of hours ESS should be designed to be capable of sustaining 50 years

It is notable from **Table 5.3** that the estimated data sample influences the multiplication factor since different expected values of wind speed and wind power are obtained. However, these values are similar, starting from a 5-year data sample. This highlights that more accurate results could be obtained using a larger data sample.

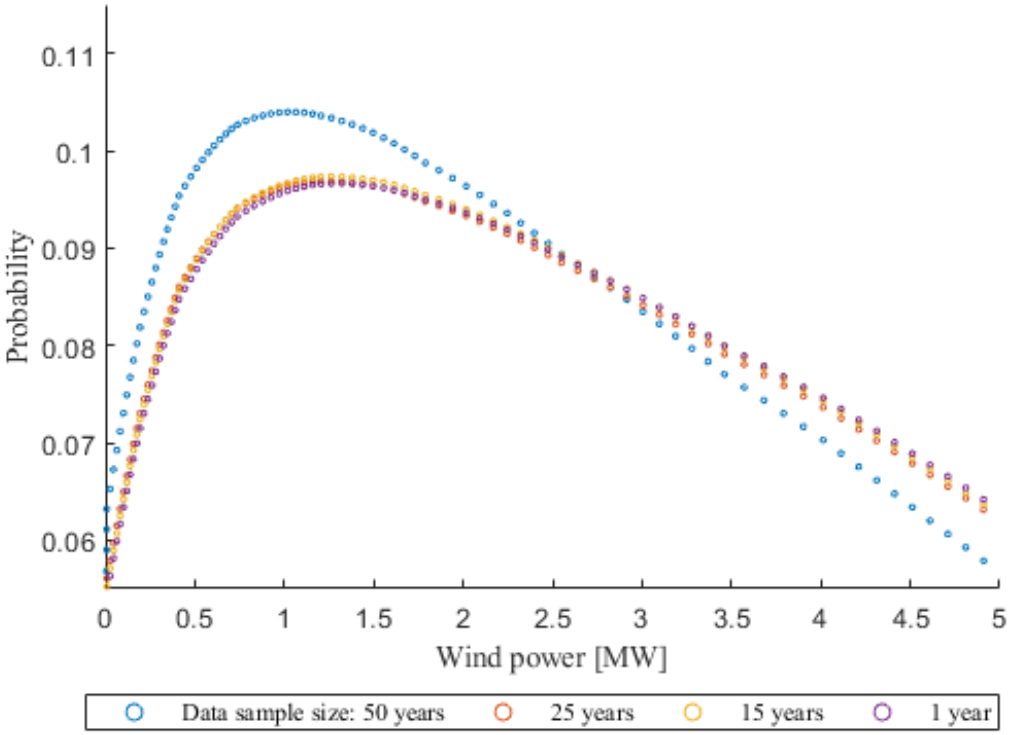

Figure 5.3 Probability of wind power supply for 50, 25, 15, 1 year.

Table 5.4 shows that the multiplication factor relies on the chosen data sample and in Method 1. For 50 years of operation, a multiplication factor equalled to 76 will be enough to estimate ESS charging. Moreover, this factor is applicable for 15 and 25 years as well. Since the data sample of 1 year is relatively small to estimate the size, correspondingly, the multiplication factor significantly differs compared to those where larger data samples are used. Moreover, window duration depends on the cut-off value; therefore, the ESS charging value will differ depending on the chosen cut-off value (**Figure 5.4**).

Table 5.4 Method 2. Sizing results. Base case.

Data sample*	**Non-productive hours****	P_{ESS}, **MW*h**	$m^{***}_{50\ yrs}$
1 year	3.7	9.4	54
15 years	2.7	6.9	74
25 years	2.6	6.7	76
50 years	2.7	6.8	76

* - data sample used for CDF calculation

- wind boundaries were scaled using **Equation 4.3, upper boundary at 10 m = 20.1 m/s, lower boundary at 10 m = 2.4 m/s

*** - multiplication factor using 50% cut-off (characteristic) value, which gives expected values of the non-productive weather window

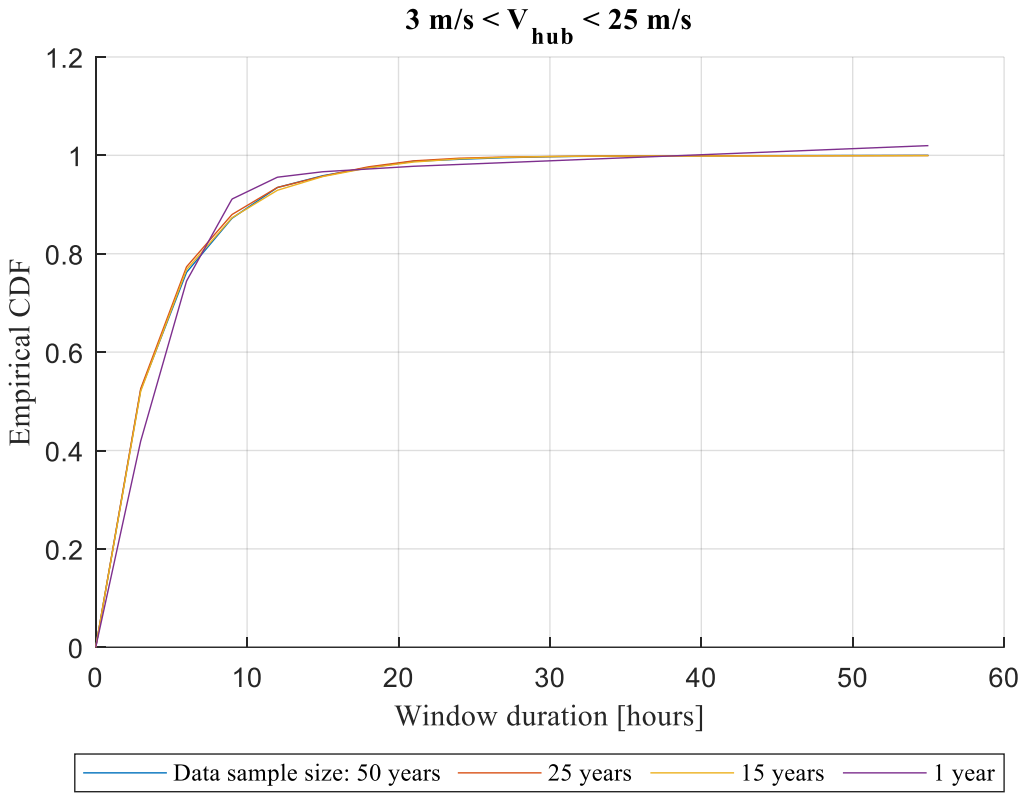

Figure 5.4 CDF function for non-productive weather windows for 50, 25, 15, and 1 year.

Method 2 is more sensitive to data sample size than Method 1. The standard deviation of the results in Method 2 equals 1.35, while in Method 1, this value equals 0.09 (**Table 5.5**). Therefore, the data sample size does not influence the wind power expected to value much.

The weather window duration explains the sensitivity of the second method to the data sample size within a particular data sample and the probability of its occurrence. More non-productive weather windows fit into the cumulative distribution function in a larger data sample. On the other hand, wind speed variation differs in different data samples, influencing the result and should be considered.

Table 5.5 Influence of the data sample size on the ESS charging result.

Data sample	P_{ESS}*, MW*h	
	Method 1**	**Method 2*****
1 year	507.0	509.8
5 years	507.2	510.2
10 years	507.0	515.0
15 years	506.8	510.6
20 years	507.0	516.0
25 years	507.2	512.0
50 years	506.6	515.8

* - operated years = 50 years, assumed as work-life of an offshore project

** - wind power expected value using different data samples

*** - CDF curve for different data samples using 50% cut-off value

Regarding the influence of the data sample size on the multiplication factor for both methods, it can be noticed from **Table 5.6** that the accuracy of the result is strongly connected with the time period chosen as a data sample. For Method 1, the factor n should be equal to at least 1000 to apply to initially estimated ESS charging. This value can vary from 1-10 percent depending on the data sample used in the investigation, wind speed variation within this data sample, and obtained wind power expected value.

For Method 2, the magnitude of the factor m depends on the cut-off value. For example, it is noticeable from **Table 5.6** that the 50 percent cut-off value requires the application of the factor m equalled to 76, for 75 percent is 36, and 95 percent is 18, respectively. Thus, it is vital to establish the applicability of the multiplication factor for different cut-off values since it will affect the final result. These observations lead to the next point, where the influence of the chosen cut-off value on the results is discussed.

Table 5.6 Influence of the data sample size on the multiplication factor.

Data sample	Multiplication factor*			
	Method 1	Method 2		
	n	$m_{50\%}$	$m_{75\%}$	$m_{95\%}$
1 year	578	54	34	18
5 years	984	70	34	14
10 years	886	72	36	14
15 years	976	74	36	16
20 years	958	74	36	14
25 years	998	76	36	16
50 years	1090	76	36	16

* - operated years = 50 years, assumed as work-life of an offshore project

Cut-off (characteristic) value

According to the simulations provided for this paper, more significant cut-off values give a more extensive duration of non-productive weather windows. It means that the total number of these windows will be such that the storage will need to be designed with a larger size. It is shown in **Table 5.7**. For cut-off values over 90 percent, ESS initial charging should be about 560 - 580 MWh. The values equal to and above 90 percent are between 510 - 540 MWh.

Table 5.7 Comparison of the results for different cut-off values.

Cut-off	$P^*_{ESS,50\ yrs}$, MW*h	$P_{ESS,25\ yrs}$, MW*h	$P_{ESS,15\ yrs}$, MWh
95%	564.8	567.8	578.2
75%	533.4	521.4	527.6
55%	520.4	513.8	507.0
50%	515.8	512.0	510.6

Moreover, the survey shows that the difference in the results for various data samples has the slightest deviation using a 50 percent cut-off value (**Table 5.8**), which gives expected values of the non-productive weather window. It means that different data sample sizes and wind speed variations give comparable values of the non-productive weather window duration on average.

Table 5.8 Standard deviation of the results for different cut-off values.

Cut-off	Standard deviation, σ
95%	12.2
90%	4.1
75%	2.8
70%	3.1
55%	2.4
50%	**1.3***

* - for data samples from 1 to 50 years

5.1.3 Applicable multiplication factor

To sum up, the results for both methods show comparable values differing from 1-10 percent depending on the data sample size and cut-off value used for the estimation. The most practical approach for Method 2 is using the expected (mean) values of weather window duration or 50 percent cut-off value, which gives comparable results regardless of which data sample size and wind speed variation are used. Since Method 1 uses wind power's expected value and data sample size does not influence much the result, the mean value of the multiplication factor for data samples from 5 to 50 years can be used. Factors are presented in **Table 5.9**.

Table 5.9 Applicable multiplication factor for Method 1 and Method 2.

Multiplication factor	
Method 1	**Method 2**
$\boldsymbol{n}$	$\boldsymbol{m}_{\mathbf{50\%}}$
1000	76

Chapter 6 – Discussions and future work

In **Chapter 6,** several important topics are dedicated to the sizing of ESS. Firstly, **Chapter 6.1** reviews the initial charging of the subsea energy storage device. Secondly, the alternative option of the power grid layout is analyzed (Ref. **Chapter 6.2**). Finally, future work is discussed (Ref. **Chapter 6.3**).

6.1 Initial charging of the device

Charging of the device from year 1 is another thing to consider. From **Figure 5.2**, charging of the ESS always faces the limits equalled to 510 MWh if it is assumed to be 50 percent charged from the start. It means that there are periods where excess power from the wind turbine is significant and can be stored in the storage device.

For the wind speed variation in the Barents Sea for 50 years, ESS should be initially charged at least 25 percent to sustain the whole operation period or maintain all the fluctuation of wind power supply and not to be empty for 50 years. The initial SoC of 25 percent is equal to 130 MWh. This value is a minimum from what ESS could start an operation, almost five times less than the 100 percent of initial SoC or 510 MWh. During the operation period, the rest of the work will be done by wind turbines and excess power. For a variation of SoC, different multiplication factors are applied using Method 1 and Method 2 (**Table 6.1**). Therefore, a smaller value of initial SoC – a smaller value of the multiplication factor is needed. The primary consideration here is manufacturing issues, which are challenging and need to be discussed.

Table 6.1 Influence of the initial charging of the ESS on the multiplication factor.

The initial state of charge (SoC) of the ESS	**Multiplication factor**	
	Method 1 - n^*	**Method 2 – $m^{**}_{50\%}$**
25 % - minimum	275	19
50 %	500	38
100 %	1100	75

* - wind expected value for 50 years

** - cut-off value = 50%

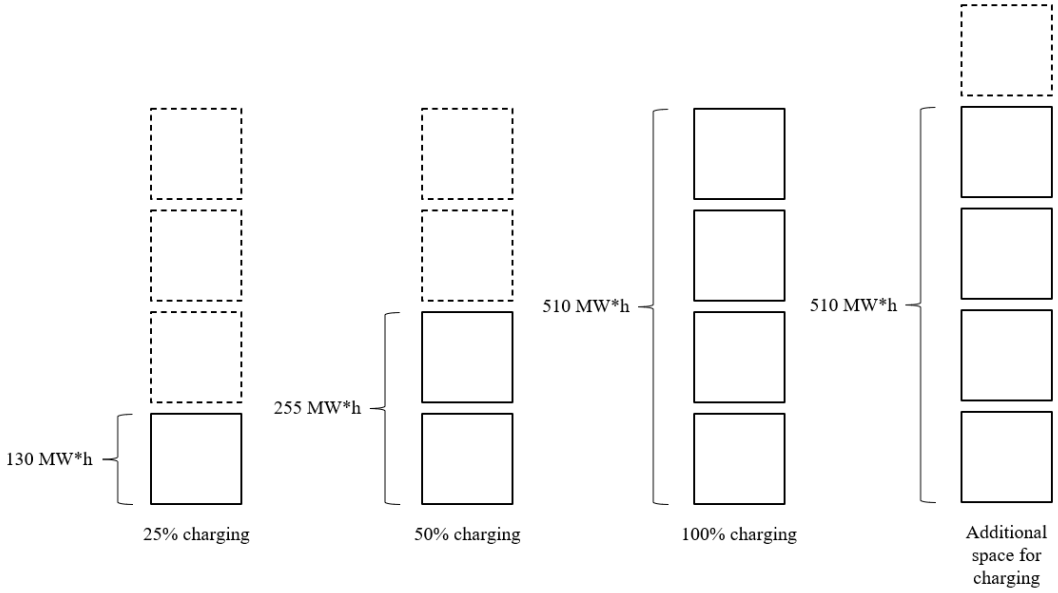

Figure 6.1 Options of device charging.

Furthermore, it can be considered to size the device with extra space for charging since excess power could be stored and utilized to reduce the renewable energy curtailment. If the size of the storage is increased by two times and will be equalled to the 1020 MWh with the same characteristics as in the base case:

- Load from the platform: 45 MW;
- Gas turbine power output: 42.5 MW;
- Number of wind turbines: 5;
- Initial SoC: 255 MWh;

It can be seen from **Table 6.2** that the mean value of SoC will shift and will be equal to 1003 MWh. It says that according to the wind speed variation in the Barents Sea for 50 years, ESS can be designed with a size of over 500 MWh and can store over 1000 MWh of energy. Such results were obtained because 70 percent of the time is a surplus of power and only 30 percent is a deficit distributed over 50 years. For more precise results and making classification that can be unique for the seas worldwide, more offshore sites and wind speed variations are needed to be considered.

Table 6.2 Mean SoC for different ESS sizes.

Size of the ESS, MW*h	Mean SoC in 50 years, MWh
510	499
1020	1003

It is a question of the economic feasibility of this proposal. It can be costly to manufacture the ESS for charging over 500 MWh. In case of additional power demand and potential expansion of the offshore project, a larger size ESS will be needed. Thus, precise calculation of the CAPEX and OPEX for the long-term operation of the hybrid energy system should be made before manufacturing the energy storage device.

6.2 Additional power supply from the shore

Since, in the base case, ESS is needed to be large enough, the question arises about what alternative solutions of power grid design can be proposed to construct the ESS in a smaller configuration with the saving of the concept with CO_2 emission decreasing and effective maintaining of power demand from the offshore facility.

To avoid the construction of large structures of subsea energy storage, the contribution from the direct power source from the shore via subsea power cable can be considered as an alternative solution. It will reduce the share of ESS's power contribution and could be implemented for the project on the continental shelf with a short step-outs (such as Laggan & Tormore (Upstreamonline, 2022), Corrib fields (Alchetron, 2022)), where the power supply technologies from the shore are already tested and widely used. Results are shown in **Table 6.4**.

The alternative solution assumes modernization of the base set-up with minimal losses of a power grid efficiency. A small size configuration of the gas turbine with a rated power of 33.3 MW was chosen (Riboldi et al., 2020) (**Table 6.3**). Power from the shore is considered the cable connected to the existing power plant onshore. Connecting to the power plant onshore will help avoid additional expenses on the required facility for power production. All the aspects mentioned above will influence several factors:

- Decrease of CO_2 emissions from the gas turbine.

- Fewer expenses on the gas turbine.
- Size decreasing of the ESS.
- Reduction of the ESS manufacturing costs.
- Reduction of the ESS installation costs.

Table 6.3 Input data. Alternative case.

Parameter	Unit	Value
Load from the offshore platform and facility	MW	45.0
Gas turbine-operated power output	MW	33.3
Power from the shore	MW	9.6
Number of wind turbines	-	5
The initial state of charge of the ESS	%	50

Table 6.4 Method 1,2. Sizing results. Alternative case.

Method	P_{ESS}*, MW*h
Method 1	360
Method 2	

* - operated years = 50 years, assumed as work-life of an offshore project

It can be seen from the results that the size of the ESS decreased by almost 30 percent compared to the base case. Instead of 500 MWh, ESS could be manufactured with a size equal to 360 MWh. Moreover, the initial SoC equals 178 MWh (50 percent initial SoC), approximately 70 MWh less than the base case, where SoC was 255 MWh. It means that power grid design can be adjusted when the smaller type of the gas turbine is used, ESS could be designed in a smaller size configuration, and HES can be connected to the already exploited power supply technology from the shore. Also, with a power cable from shore, any excess power from WT could be exported back to the grid.

6.3 Future work

According to the background presented above, several points could be analyzed in future work. Firstly, wind speed data for the North and Norwegian Seas should be considered to establish

the size of the ESS applicable on the whole territory of the Norwegian continental shelf. In addition, worldwide long-term wind data for the seas can be studied to classify the ESS size for different areas. Secondly, Machine Learning tools for wind data analysis could be applied in future investigations to more precisely determine weather windows, their duration, and mean wind speed values. Moreover, it will help study the data sample and cut-off (characteristic) value influence on the final result and identify the data that will be most accurate for sizing. Finally, studies on installing the ESS with large sizes offshore could be conducted with an assumption about decreasing the contribution of the gas turbines having the most significant share of CO_2 emissions in the power grid of the hybrid energy system. All recommendations can help create HES using ESS with the lowest emissions rate into the atmosphere and highest power efficiency.

Chapter 7 - Conclusions

This master's thesis proposes a methodology for sizing subsea energy storage devices for offshore wind-powered oil and gas platforms. It consists of 2 methods. The first method uses the Weibull distribution function to estimate the wind speed expected value. The second method relies on the weather window analysis considering weather windows without wind power contribution. Both methods aim to estimate the ESS size capable of operating within a chosen time period in the hybrid energy system, consisting of the offshore platform, wind farm as a renewable energy source, and non-renewable energy source (such as gas turbine). As an alternative solution, a power supply from the shore by the subsea power cable was proposed. The results show that subsea energy storage of a considerable size equalled to 500 MWh is required for 50 years of exploitation.

Furthermore, both methods are applicable for sizing since they show comparable results. In addition, data sample size does not influence the final sizing result and multiplication factor of method 1. This is mainly because the mean wind speed in different time intervals is approximately the same.

On the other hand, for method 2, sizing results differ by 2 percent due to a different number of weather windows within a particular data sample. What is more, the sizing result is affected by chosen cut-off (characteristic) value. The difference in the results can be 12 percent, depending on the selected value. It is considered that the 50 percent cut-off value is more applicable since it is the most common option within the assumed time frame. Finally, it must be mentioned that the initial state of charge of the device should be at least 25 percent to operate, and the maximum size of the device could be expanded to more than 500 MWh in the Barents Sea wind conditions. This study is expected to be used as a guide for planned and existing projects regarding sizing subsea energy storage.

References

Aardal, A. R., Marvik, J. I., Svendsen, H., & Tande, J. O. G. (2012). Study of offshore wind as power supply to oil and gas platforms. Offshore Technology Conference,

Agbossou, K., Kolhe, M., Hamelin, J., & Bose, T. K. (2004). Performance of a stand-alone renewable energy system based on energy storage as hydrogen. *IEEE Transactions on energy conversion*, *19*(3), 633-640. https://doi.org/10.1109/Tec.2004.827719

Alchetron. (2022). *Corrib gas project*. https://alchetron.com/Corrib-gas-project#corrib-gas-project-f89b5572-a22e-4ee9-b304-bbd6b33289d-resize-750.jpeg

Bitner-Gregersen, E. M. (2005). Joint probabilistic description for combined seas. International Conference on Offshore Mechanics and Arctic Engineering,

Bitner-Gregersen, E. M., & Haver, S. (1991). Joint environmental model for reliability calculations. The First International Offshore and Polar Engineering Conference,

Budt, M., Wolf, D., Span, R., & Yan, J. (2016). A review on compressed air energy storage: Basic principles, past milestones and recent developments. *Applied Energy*, *170*, 250-268.

Cha, H. J., & Enjeti, P. N. (2003). A three-phase AC/AC high-frequency link matrix converter for VSCF applications. IEEE 34th Annual Conference on Power Electronics Specialist, 2003. PESC'03.,

Chen, L., Liu, Y., Arsoy, A., Ribeiro, P., Steurer, M., & Iravani, M. (2006). Detailed modeling of superconducting magnetic energy storage (SMES) system. *IEEE Transactions on Power Delivery*, *21*(2), 699-710.

Davide, M., Riccardo, M., & Andreas, U. (2016). JRC Ocean Energy Status Report: 2016 Edition.

Dincer, I., Cozzani, V., & Crivellari, A. (2021). *Hybrid Energy Systems for Offshore Applications*. Elsevier.

EMEC. (2020a). *Classification of Tidal Energy devices 2020*. http://www.emec.org.uk/marine-energy/tidal-devices/

EMEC. (2020b). *Classification of Wave Energy devices 2020*. http://www.emec.org.uk/marine-energy/wave-devices/

Eriksen, R., Engel, D., Haugen, U., Hodne, T., Hovem, L., Alvik, S., & Rinaldo, M. (2021). DNV AS: Energy Transition Outlook 2021 - Technology Progress Report. https://www.dnv.com/Publications/energy-transition-norway-2021-212201

Europe, W. (2018). *Offshore wind in Europe offshore wind in Europe*.

Global Wind Energy Council. (2017). GWEC Global Wind Report 2019. *Global Wind Energy Council: Bonn, Germany*.

Hahn, H., Hau, D., Dick, C., & Puchta, M. (2017). Techno-economic assessment of a subsea energy storage technology for power balancing services. *Energy*, *133*, 121-127.

He, W., Jacobsen, G., Anderson, T., Olsen, F., Hanson, T. D., Korpås, M., Toftevaag, T., Eek, J., Uhlen, K., & Johansson, E. (2010). The potential of integrating wind power with offshore oil and gas platforms. *Wind Engineering*, *34*(2), 125-137.

He, W., Uhlen, K., Hadiya, M., Chen, Z., Shi, G., & del Rio, E. (2013). Case study of integrating an offshore wind farm with offshore oil and gas platforms and with an onshore electrical grid. *Journal of Renewable Energy*, *2013*.

Husain, A. A., Hasan, W. Z. W., Shafie, S., Hamidon, M. N., & Pandey, S. S. (2018). A review of transparent solar photovoltaic technologies. *Renewable and Sustainable Energy Reviews*, *94*, 779-791.

Hut, L. (2020). *Investigating the structural behaviour of the Ocean Battery*

IRENA, A. (2019). Renewable energy statistics 2019. *Abu Dhabi, United*.

Islam, M. T., Huda, N., Abdullah, A., & Saidur, R. (2018). A comprehensive review of state-of-the-art concentrating solar power (CSP) technologies: Current status and research trends. *Renewable and Sustainable Energy Reviews*, *91*, 987-1018.

Jonkman, J., Butterfield, S., Musial, W., & Scott, G. (2009). *Definition of a 5-MW reference wind turbine for offshore system development*.

Jurasz, J., Mikulik, J., Krzywda, M., Ciapała, B., & Janowski, M. (2018). Integrating a wind- and solar-powered hybrid to the power system by coupling it with a hydroelectric power station with pumping installation. *Energy*, *144*, 549-563.

Kaldellis, J., Kapsali, M., & Kavadias, K. (2010). Energy balance analysis of wind-based pumped hydro storage systems in remote island electrical networks. *Applied Energy*, *87*(8), 2427-2437.

Kapsali, M., & Kaldellis, J. (2010). Combining hydro and variable wind power generation by means of pumped-storage under economically viable terms. *Applied Energy*, *87*(11), 3475-3485.

Khan, J., & Arsalan, M. H. (2016). Solar power technologies for sustainable electricity generation–A review. *Renewable and Sustainable Energy Reviews*, *55*, 414-425.

Kies, A., Schyska, B., Viet, D. T., von Bremen, L., Heinemann, D., & Schramm, S. (2017). Large-scale integration of renewable power sources into the Vietnamese power system. *Energy Procedia*, *125*, 207-213.

Kloster, E. K. H., Tonnessen, S. M., & Akritidis, A. (2021). *Subsea energy storage*.

KonKraft. (2020). *The energy industry of tomorrow on the Norwegian continental shelf*. https://www.norskoljeoggass.no/contentassets/19ca8199a3b5459f850b1624ad0ee1c6/the-energy-industry-of-tomorrow-on-the-ncs----konkraft-report-2021-2.pdf

Korpås, M., Warland, L., He, W., & Tande, J. O. G. (2012). A case-study on offshore wind power supply to oil and gas rigs. *Energy Procedia*, *24*, 18-26.

Legorburu, I., Johnson, K. R., & Kerr, S. A. (2018). Multi-use maritime platforms-North Sea oil and offshore wind: Opportunity and risk. *Ocean & Coastal Management*, *160*, 75-85.

Li, L., Gao, Z., & Moan, T. (2015). Joint distribution of environmental condition at five european offshore sites for design of combined wind and wave energy devices. *Journal of Offshore Mechanics and Arctic Engineering*, *137*(3).

Li, L., Zhu, X., Parra, C., & Ong, M. C. (2021). Comparative study on two deployment methods for large subsea spools. *Ocean Engineering*, *233*, 109202.

Lundin, R., & Beitler-Dorch, B. (2018). Modelling and Analysis of Mobile Energy Transmission for Offshore Wind Power: An analysis of flow batteries as an energy transmission system for offshore wind power.

Maharjan, L., Inoue, S., & Akagi, H. (2008). A transformerless energy storage system based on a cascade multilevel PWM converter with star configuration. *IEEE Transactions on Industry Applications*, *44*(5), 1621-1630. https://doi.org/10.1109/Tia.2008.2002180

Nehrir, M. H., Wang, C., Strunz, K., Aki, H., Ramakumar, R., Bing, J., Miao, Z., & Salameh, Z. (2011). A Review of Hybrid Renewable/Alternative Energy Systems for Electric Power Generation: Configurations, Control, and Applications. *Ieee Transactions on Sustainable Energy*, *2*(4), 392-403. https://doi.org/10.1109/Tste.2011.2157540

Nguyen, T.-V., Barbosa, Y. M., da Silva, J. A., & de Oliveira Junior, S. (2019). A novel methodology for the design and optimization of oil and gas offshore platforms. *Energy*, *185*, 158-175.

Nguyen, T.-V., Voldsund, M., Breuhaus, P., & Elmegaard, B. (2016). Energy efficiency measures for offshore oil and gas platforms. *Energy*, *117*, 325-340.

Norwegian government. (2019). *Regjeringa legg fram Noregs lågutsleppsstrategi for 2050. Regjeringen*. https://www.regjeringen.no/no/dokumentarkiv/regjeringen-solberg/aktuelt-regjeringen-solberg/kld/nyheter/2019-nyheter/regjeringa-legg-fram-noregs-lagutsleppsstrategi-for-2050/id2672248/

Norwegian Petroleum. (2022). *Emissions to air*. https://www.norskpetroleum.no/en/

Orlandini, V., Pierobon, L., Schløer, S., De Pascale, A., & Haglind, F. (2016). Dynamic performance of a novel offshore power system integrated with a wind farm. *Energy*, *109*, 236-247.

Our World in Data. (2022). *CO_2 and Greenhouse Gas Emissions*. https://ourworldindata.org/air-pollution

Papaefthymiou, S. V., & Papathanassiou, S. A. (2014). Optimum sizing of wind-pumped-storage hybrid power stations in island systems. *Renewable energy*, *64*, 187-196.

Rafiee, A., & Khalilpour, K. R. (2019). Renewable hybridization of oil and gas supply chains. In *Polygeneration with polystorage for chemical and energy hubs* (pp. 331-372). Elsevier.

Rahman, S., & Tam, K. S. (1988). A Feasibility Study of Photovoltaic-Fuel Cell Hybrid Energy System. *IEEE Transactions on energy conversion*, *3*(1), 50-55. https://doi.org/Doi 10.1109/60.4199

Reistad, M., Breivik, Ø., Haakenstad, H., Aarnes, O. J., Furevik, B. R., & Bidlot, J. R. (2011). A high-resolution hindcast of wind and waves for the North Sea, the Norwegian Sea, and the Barents Sea. *Journal of Geophysical Research: Oceans*, *116*(C5).

Riboldi, L., Alves, E. F., Pilarczyk, M., Tedeschi, E., & Nord, L. O. (2020). Optimal design of a hybrid energy system for the supply of clean and stable energy to offshore installations. *Frontiers in Energy Research*, *8*, 346.

Riboldi, L., & Nord, L. O. (2018). Offshore power plants integrating a wind farm: design optimization and techno-economic assessment based on surrogate modelling. *Processes*, *6*(12), 249.

Riboldi, L., Völler, S., Korpås, M., & Nord, L. O. (2019). An integrated assessment of the environmental and economic impact of offshore oil platform electrification. *Energies*, *12*(11), 2114.

Rourke, F. O., Boyle, F., & Reynolds, A. (2010). Tidal energy update 2009. *Applied Energy*, *87*(2), 398-409.

Roussanaly, S., Aasen, A., Anantharaman, R., Danielsen, B., Jakobsen, J., Heme-De-Lacotte, L., Neji, G., Sødal, A., Wahl, P. E., & Vrana, T. K. (2019). Offshore power generation with carbon capture and storage to decarbonize mainland electricity and offshore oil and gas installations: A techno-economic analysis. *Applied Energy*, *233*, 478-494.

Sahu, A., Yadav, N., & Sudhakar, K. (2016). Floating photovoltaic power plant: A review. *Renewable and Sustainable Energy Reviews*, *66*, 815-824.

Slocum, A. H., Fennell, G. E., Dundar, G., Hodder, B. G., Meredith, J. D., & Sager, M. A. (2013). Ocean renewable energy storage (ORES) system: Analysis of an undersea energy storage concept. *Proceedings of the IEEE*, *101*(4), 906-924.

Statistics Norway. (2021). *Emissions to air. Statistisk Sentralbyrå*. https://www.ssb.no/en/natur-og-miljo/forurensning-og-klima/statistikk/utslipp-til-luft

Upstreamonline. (2022). *More big impairments for Total in UK*. https://www.upstreamonline.com/online/more-big-impairments-for-total-in-uk/2-1-435618

Zhang, H., Baeyens, J., Degrève, J., & Cacères, G. (2013). Concentrated solar power plants: Review and design methodology. *Renewable and Sustainable Energy Reviews*, *22*, 466-481.

Appendix A – MATLAB code

```
%full script for analysis
clc; clear all; close all;
%cd("C:\Users\264662\Universitetet i Stavanger\Kirill Krotov's MSc thesis - Documents\General\Paper 1. Optimal design\LTA");

%Wind data

data_all = load('WAM10_7202N_2210E_cut.txt'); %Data from Lin - Barents sea - 50 years
data_all2 = data_all;
```

Method 1 - Wind speed expected value

```
%Step 1 (a)
```

Offshore grid design

```
Load =  45 %Load from the offshore platform

%2 comparable GTs
GT_turbine = str2double( 44.7 ) %power supply from gas turbine
GT_workload = 0.95 %power rate of gas turbine
GT = GT_turbine*GT_workload

WT_num =  5 %number of wind turbines

int = [unique(data_all(:,1)) (0:49)']; %assign to each date particular multiplicator
Start_date = str2double( 1961 )
End_date = str2double( 2010 )
Timeframe = End_date - Start_date %timeframe in years

%find the multiplicator for date to find corresponding values of wind speed in the notepad
indices1 = find(int(:,1) == Start_date);
m1 = int(indices1,2);

if Start_date == 1961
    ts = 1;
else
    ts = 2920*m1;
end

indices2 = find(int(:,1) == End_date);
m2 = int(indices2,2);

if End_date == 1961
    te = 1;
else
    te = 2920*m2;
end

first_last_row = [ts, te]
```

Weibull ditribution of wind speed over 50 years

```
ws_data = reshape(data_all2(1:(te-(ts-1)),5),[1,(te-(ts-1))])  %wind speed data for chosen timeframe

% 2 parameter Weibull
[a1, b1] = func_Wei2_fit(ws_data, 'MLE') %a-scale, b-shape
y_weibull = wblpdf(ws_data,a1,b1)

scatter(ws_data,y_weibull,4,"o")
xlabel('Wind speed [m/s]', "FontName",'times')
ylabel('Probability', "FontName",'times')
legend(string(Timeframe) + ' years', "FontName",'times')

[ws_expected_value,variance] = wblstat(a1,b1) %return mean and variance from weibull distribution
%NREL 5 MW - power=f(probability)
k = load('nrel5mw.mat');

%Data for NREL 5MW wind turbine
WT_data = [k.nrel5mw(:,1),k.nrel5mw(:,2),k.nrel5mw(:,3)];
colNames = {'Wind speed [m/s]','Probability','Power from WT [MW]'};
WT_data_table = array2table(WT_data,'VariableNames',colNames)

X = k.nrel5mw(:,3);
YY = k.nrel5mw(:,1);
%% Fit: 'Wind speed and Power'.
[xData, yData] = prepareCurveData( YY, X );

% Set up fittype and options.
ft = 'linearinterp';

% Fit model to data.
[fitresult, gof] = fit( xData, yData, ft, 'Normalize', 'on' );

% Plot fit with data.
figure( 'Name', 'Wind speed and Power' );
h = plot( fitresult,  xData, yData);
% Label axes
xlabel( 'Wind speed [m/s]', 'Interpreter', 'none' , "FontName",'times');
ylabel( 'Power from WT [MW]', 'Interpreter', 'none' , "FontName",'times');
legend("FontName",'times')

vq1 = interp1(k.nrel5mw(:,1),k.nrel5mw(:,2),ws_expected_value); %interpolated value of wind speed probability
vq2 = interp1(k.nrel5mw(:,1),k.nrel5mw(:,3), ws_expected_value); %interpolated value of wind power probability

wp_expected_value = vq2
```

Power demand equation - using Expected Value

```
WT = wp_expected_value

syms Y
ESS_init = double(solve(Load - GT - WT - Y == 0, Y))
```

Method 2 - Weather window duration and CDF function plot

```
f10 = figure(10); set(f10,'Position',[150 150 400 250]);

% dataset_1year = data_all2(1:2920, :); %taking the data from the year 1961

%Boundary values of the wind speed, where there is no production 3 and 25
%m/s
%Scaling fucntion - u(z) = U10 * (z/10)^alpha, z - height, alpha - exponent

z = 90; %height, where the wind speed was measured - hub height
alpha = 0.1; %exponent

max_ws_10m = 25/((z/10)^alpha) %25 m/s
min_ws_10m = 3/((z/10)^alpha) %3 m/s

plot(1:(te-(ts-1)),data_all2(ts:te,5))
ylabel('Wind speed [m/s]', "FontName",'times')
xlabel ('Time [Years]', "FontName",'times')
 xticks([14600 29200 43800 58400 73000 87600 102200 116800 131400 143080])
    xticklabels({'5','10','15','20','25','30','35','40','45','50'})
    xlim([0 143080])
hold on
yline(max_ws_10m,'--r', {'Max'}, "FontName",'times')

hold on
yline(min_ws_10m,'--r', {'Min'}, "FontName",'times')

hold off

Hs_total_min = 0;
wind_total_lim = [max_ws_10m;min_ws_10m];     % Limitis, where there is no power production

% find the data for ws_total < a max value
       index_ws_total = (or(data_all2(ts:te,5)<=wind_total_lim(2), data_all2(ts:te,5)>=wind_total_lim(1)));
       index_window = zeros(size(index_ws_total)); % vector to count for the window length

 %Actually this calculator summarize TRUEs of condition (1+1+1 ... = n) before it is FALSE (0), and store it in the array
       for ii = 1:1:length(data_all2(ts:te,5))

           if ii == 1 && (index_ws_total(ii)==1)        % the first data in the history
               m_count = 0;
               for jj=1:1:length(data_all2(ts:te,5))
                   if index_ws_total(jj) == 1
                       m_count=m_count+1;
                   else
                       break
                   end

                   index_window(ii) = m_count;         % number of events within the window

               end
           elseif ii == 1 && (index_ws_total(ii)==0)
               index_window(ii) =0;

           elseif ((index_ws_total(ii-1)==0) && (index_ws_total(ii)==1))
               m_count = 0;
               for jj=ii:1:length(data_all2(ts:te,5))           % count for the weather windows with index =1
                   if index_ws_total(jj) == 1
                       m_count=m_count+1;
                   else
                       break
                   end

                   index_window(ii) = m_count;          % count for the weather windows with index =1
               end
           end
       end
```

```
  % plot empirical CDF of weather windows

        w_window = index_window(index_window>0)*3;  % the data is 3-hour data
        case1_sort = sort(w_window);
        no_window = length(w_window)   % number of windows per year
        duration_window = mean(w_window) % mean duration of window
        cdf_emp = (1:1:length(case1_sort))/(length(case1_sort)+1);   % empirical CDF

        % remove repeating points in the plot
        changedIndexes = diff(case1_sort)~=0;
        Indexes = find(changedIndexes == 1);
        Indexes = [Indexes', length(case1_sort)];
        case1_sort2 = case1_sort(Indexes);
        f_dist = cdf_emp(Indexes);

%         figure(10); subplot(2,1,kk);
        plot(case1_sort2, f_dist, 'bo','MarkerSize', 3); grid on;
        figure(10);  title(['Wind speed <= ' num2str(min_ws_10m) ' m/s and >= ' num2str(max_ws_10m) ' m/s'], "FontName",'times'); xlim([0 55]); ylim([0 1]);
        ylabel('Empirical CDF', "FontName",'times'); xlabel('Window duration [hours]', "FontName",'times');
        legend(string(Timeframe) + ' years','Location', 'SouthEast', "FontName",'times');

%interpolating data for CDF
[xData, yData] = prepareCurveData( case1_sort2, f_dist );

% Set up fittype and options.
ft = 'linearinterp';

% Fit model to data.
[fitresult, gof] = fit( xData, yData, ft, 'Normalize','on' );

% Plot fit with data.
h = plot(fitresult);
```

```
 % Get the handle to the fitted curve
 curveHandle = findobj(h,'DisplayName', 'fitted curve');
 % Get the X and Y values Matlab chose
 x_extracted = curveHandle.XData;
 y_extracted = curveHandle.YData;

 xlim([0 55]); ylim([0.4 1]);
 title(['3 m/s < V_h_u_b < 25 m/s'], "FontName",'times');
 % Label axes
 xlabel( 'Window duration [hours]', "FontName",'times');
 ylabel( 'Empirical CDF', "FontName",'times' );
 legend(string(Timeframe) + ' years','Location', 'SouthEast', "FontName",'times')
 grid on
        clear index_ws_total
 %     end
 % end
```

ESS capacity depending on non-productive hours

```
%cdf_function = [case1_sort2 f_dist'];
%cdf_function_table = array2table(cdf_function,'VariableNames',{'Window duration (hours)' 'CDF value'})

cdf_function = [x_extracted' y_extracted'];
cdf_function_table = array2table(cdf_function,'VariableNames',{'Window duration (hours)' 'CDF value'})

prob = str2double( 0.5 )
vq10 = interp1(cdf_function_table.("CDF value"),cdf_function_table.("Window duration (hours)"),prob); %interpolated value of window duration

no_production_hours = vq10

init_ess_capacity = (Load-GT)*no_production_hours
% nn = cdf_function(cdf_function(:,2) <= prob,1);
% no_production_hours = nn(end)

% factor =  6
```

Checking ESS size over 50 years for Method 2

```
wind_speed = data_all(ts:te,5);

vq3 = interp1(k.nrel5mw(:,1),k.nrel5mw(:,2),wind_speed); %interpolated value of wind speed probability
vq4 = interp1(k.nrel5mw(:,1),k.nrel5mw(:,3), wind_speed); %interpolated value of wind power probability

wind_power = vq4; %interpolated values of wind power
wind_power(isnan(wind_power)) = 0; %replace all NaNs with zeroes, where it can not be interpolated

wind_power_table = array2table([wind_speed wind_power],'VariableNames',{'Wind speed [m/s]' 'Wind power [MW]'})
ess_capacity = zeros(size(wind_power));
energy = zeros(size(wind_power));

factor = 0;
empty_hours = 1;

while empty_hours > 0

      factor = factor + 1;
      ess_capacity_MW = (Load-GT)*no_production_hours * factor; %no wind power production
      ess_capacity(1) = ess_capacity_MW;

    for i = 2:(te-(ts-1))

          energy(i) = (WT_num*wind_power(i) + GT - Load) * 3;
    ess_capacity(1) = ess_capacity_MW;

    if ess_capacity(i-1) + energy(i) > 2*ess_capacity_MW
         ess_capacity(i) =  2*ess_capacity_MW;
        else if ess_capacity(i-1) + energy(i) <= 0
            ess_capacity(i) = 0;
        else
     ess_capacity(i) = ess_capacity(i-1) + energy(i);
        end
    end

    end
    empty_hours = nnz(ess_capacity == 0)*3;
end
%Table
energy_table = array2table([energy wind_power ess_capacity] ,'VariableNames',{'Total energy' 'Wind power in every 3 hour' 'ESS capacity'})
sum(energy<0)
sum(energy>0)

%Figure
f1 = figure;
f1.Position = [500 100 600 600];
plot(1:te-(ts-1), ess_capacity)
title ('Period: ' + string(Start_date) + '-' + string(End_date) + ', ' + string(Timeframe) + ' years', "FontName",'times')
xlim([0 te-(ts-1)])
xlabel('Time [3 hours]', "FontName",'times')
ylabel('ESS charging [MW*h]', "FontName",'times')
text(mean(0:te-(ts-1)), 0.2*max(ess_capacity), {'Initial: ' + string(ess_capacity_MW), 'Max: ' + string(max(ess_capacity)), 'Mean: ' ...
    + string(mean(ess_capacity)), 'End cap.: ' + string(ess_capacity(end))}, "FontName",'times')

ess_capacity_MW
factor
empty_hours
total_hours = (te-(ts-1)) * 3
```

Checking ESS size over 50 years for Method 1

```
ess_capacity2 = zeros(size(wind_power));
energy2 = zeros(size(wind_power));


    factor2 = 0;
    empty_hours2 = 1;

    while empty_hours2 > 0

        factor2 = factor2 + 1;
        ESS = ESS_init * factor2;
        ess_capacity2(1) = ESS;

        for i = 2:(te-(ts-1))
            energy2(i) = (WT_num*wind_power(i) + GT - Load) * 3;
                if ess_capacity2(i-1) + energy2(i) > 2*ESS
                   ess_capacity2(i) =  2*ESS;
                    else if ess_capacity2(i-1) + energy2(i) <= 0
                            ess_capacity2(i) = 0;
                    else
                            ess_capacity2(i) = ess_capacity2(i-1) + energy2(i);
                    end
                end
        end
        empty_hours2  = nnz(ess_capacity2 == 0)*3;
     end

%Table
energy_table2 = array2table([energy2 wind_power ess_capacity2] ,'VariableNames',{'Total energy' 'Wind power in every 3 hour' 'ESS capacity'})
```

```
%Figure
f2 = figure;
f2.Position = [500 100 600 600];
plot(1:te-(ts-1), ess_capacity2, 'Color','r')
title ('Period: ' + string(Start_date) + '-' + string(End_date) + ', ' + string(Timeframe) + ' years', "FontName",'times')
xlim([0 te-(ts-1)])
xlabel('Time [3 hours]', "FontName",'times')
ylabel('ESS charging [MW*h]', "FontName",'times')
text(mean(0:te-(ts-1)), 0.2*max(ess_capacity2), {'Initial: ' + string(ESS), 'Max: ' + string(max(ess_capacity2)), 'Mean: ' ...
    + string(mean(ess_capacity2)), 'End cap.: ' + string(ess_capacity2(end))}, "FontName",'times')

ESS
factor2
empty_hours2
total_hours
```

Appendix B – Paper draft

A methodology for sizing subsea energy storage devices for offshore wind-powered oil and gas platforms

Kirill Krotov[1], Yihan Xing[1,*], Lin Li[1], Rasmus Juhlin[2], Xiaosen Xu[3]

[1] University of Stavanger, Norway

[2] Subsea 7 Norway AS, Norway

[3] Jiangsu University of Science and Technology, Zhenjiang, China

1 Introduction

Traditional offshore field development is always connected with emissions such as CO_2 and greenhouse gases, taking up 5.8% of worldwide emissions [1]. Air pollution contributes to global warming. From November 1982 to February 2022 global temperature anomaly increased by 0.72 °C [1]. For instance, in Norway, from 2019 to 2020, greenhouse gas emissions from petroleum activities corresponded to about 12.5 million tonnes of carbon dioxide equivalent. Still, emissions decreased by 3.5% compared to 1990-2020, where the number of emissions reduced only by 4.2% [1][2]. According to DNV and the Federation of Norwegian Industries Energy Transition, Norway's outlook reports that emissions will be reduced by 24% by 2030 and 79% by 2050 compared to 1990 [3]. On the other hand, in February 2020 Norwegian government updated the goal of reducing emissions by at least 50% and towards 55% below 1990 levels by 2030 [4]. Such optimistic forecasts are possible due to modern approaches for reducing emissions into the atmosphere and providing a sustainable and clean energy supply capable of meeting power demand from offshore facilities, described by KonKraft [5], including the projects connected with electrification [6], energy efficiency measures [7], carbon capture and storage [8], and design optimisation of the platform [9].

A promising approach is the hybrid energy system (HES). It is a concept, which comprises utilising traditional power generation technologies, such as gas turbines and onshore power sources, in conjunction with renewable energy sources (wind, solar, and hydropower) and energy storage technologies located on-site, onshore, or subsea. A hybrid offshore renewable energy platform that comprises wind turbines and arrays of wave energy converters was proposed by Hanssen [12], which is unique in this area, providing beneficial technical results and economic performance for the North Sea. Rafiee and Khalilpour [16] provided an overview of various applications of renewable energy sources in the oil and gas sector, focusing on the hybridisation and highlighting that integration of clean energy sources with the petroleum industry decreases not only its emissions intensity but production costs. Among other clean energy sources, the wind is the most developed and most promising, making significant progress in the oil and gas industry regarding emissions reduction compared to solar and hydropower. Hence, more attention is paid to wind power integration into a power grid system of offshore platforms. There are already investigations of the integration of wind power to either simple cycle gas turbines [13][20] and into the onshore grid [21], or offshore power systems integrated with a wind farm providing optimisation and techno-economic assessment [14][15]. The viability of proposed strategies is influenced by increased costs on the integration of wind power systems into offshore installations [22] and proper estimation of excess wind power potential. Adding the energy storage part to the power demand equation could be a helpful solution for handling the irregularity of wind power, valuability of its integration into the hybrid energy system, and utilising the wide potential of wind excess power.

Nowadays, there are a variety of energy storage inventions successfully implemented into the hybrid energy system, such as electrolysers proposed by Riboldi [22], subsea energy storage by Kloster [23], and subsea

tanks by Fraunhofer Institute [35] and Massachusetts Institute of Technology (MIT) [36]. Integration of the subsea energy storage into the power grid of HES implies its interconnection with wind energy. Since the wind is intermittent, wind turbines cannot consistently supply power and match the power demand. Wind power output is strongly connected with the wind irregularity, which means that energy storage system (ESS) power contribution is also connected with it. Depending on wind power output, the ESS will provide or store power. Therefore, the ESS charging will not be constant during the operation period; there will be fluctuations in the charging. Thus, the ESS must be designed in such a way as to be capable of sustaining these fluctuations in power demand. In other words, it should be appropriately sized.

This paper proposes a methodology for sizing an ESS integrated into the hybrid energy system. When it is planned to design HES in conjunction with a wind farm or execute a part of power contribution from the HES (for instance, change the configuration of the gas turbine to a smaller one) and fill this gap with an energy storage device, a suitable sizing method is required. Since there are several approaches to analysing the wind data, two methods for ESS sizing are established in this study using 50 years of wind data from the Barents Sea [42]. The first method is based on estimating the design ESS size required using the expected wind speed value (Section 3.2). The second method estimates the design ESS size using weather windows (Section 3.3). This parameter shows the number of weather windows without wind power output due to wind speed exceeding or below operational boundaries of the wind turbine. Results from these method then are tested through actual historical wind data, where multiplication factor is empirically feeded to adjust the ESS design to the minimum required size capable to operate within assumed operational period (Section 0). The aim is to increase understanding of the excess wind power potential and its cooperation with an energy storage device, effectively integrating ESS into a hybrid system by applying the proposed methodology, avoiding unnecessary costs, energy losses, and emissions into the atmosphere. This paper presents the first publicly available methodology for subsea energy storage device sizing using long-term wind data to the authors' best knowledge.

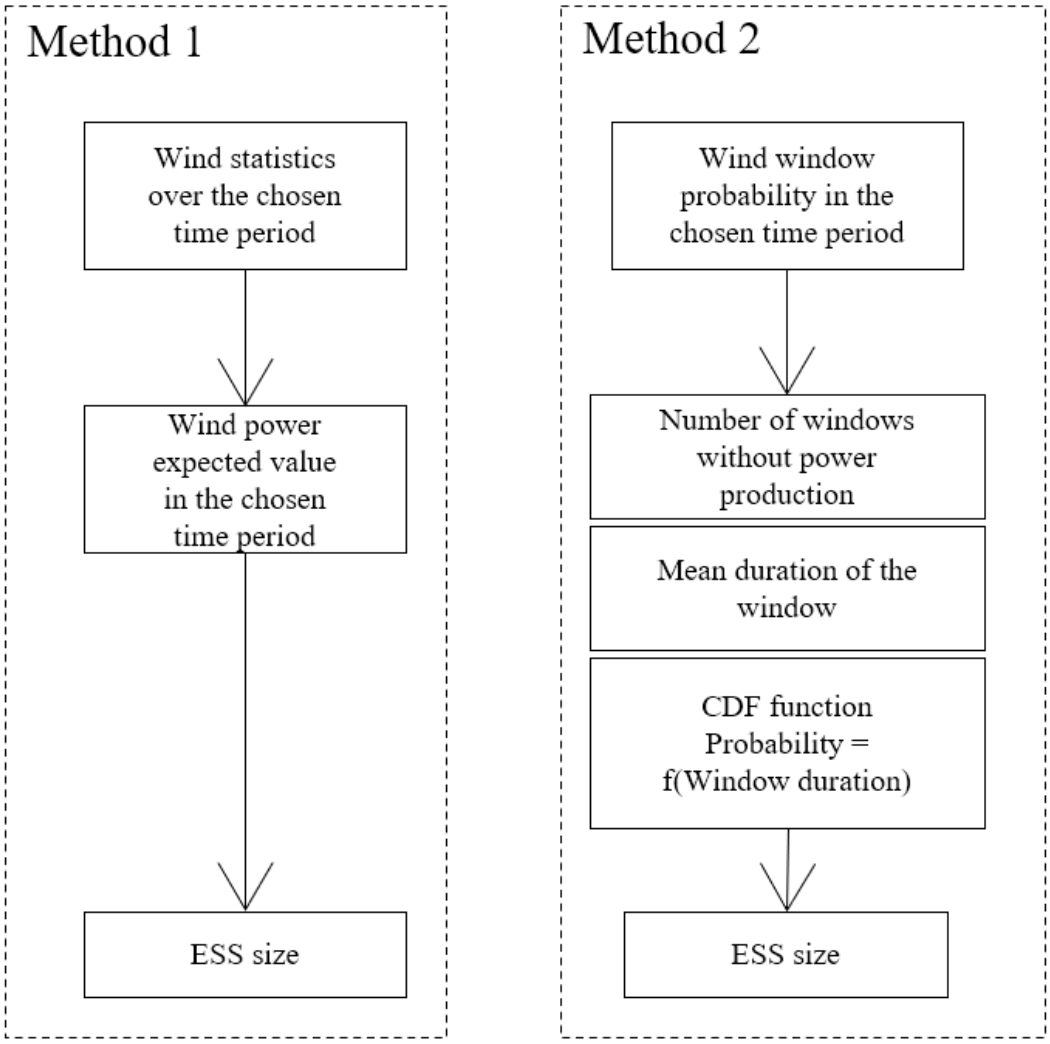

Figure 1 R&D approach scheme.

2 System description

2.1 Hybrid energy system

The hybrid energy system for offshore oil and gas platforms combines an energy storage device, gas turbines, an offshore wind farm, and power from shore. The primary power supply is gas turbines (GTs) and/or onshore power sources. These provide the base-load power to the offshore installations. The offshore wind farm and ESS provide the remaining power. In case of excess power from the wind turbine, it is stored in the ESS and used when needed. Conversely, ESS supplies the required amount of power in the lack of wind power. Figure 2 presents a schematic of the HES, where one of the ESS concepts is shown.

There are several options for how power can be supplied to the offshore facility:

1. Gas turbine + Wind farm + ESS
2. Onshore power + Wind farm + ESS
3. Gas turbine + Onshore power + Wind farm + ESS

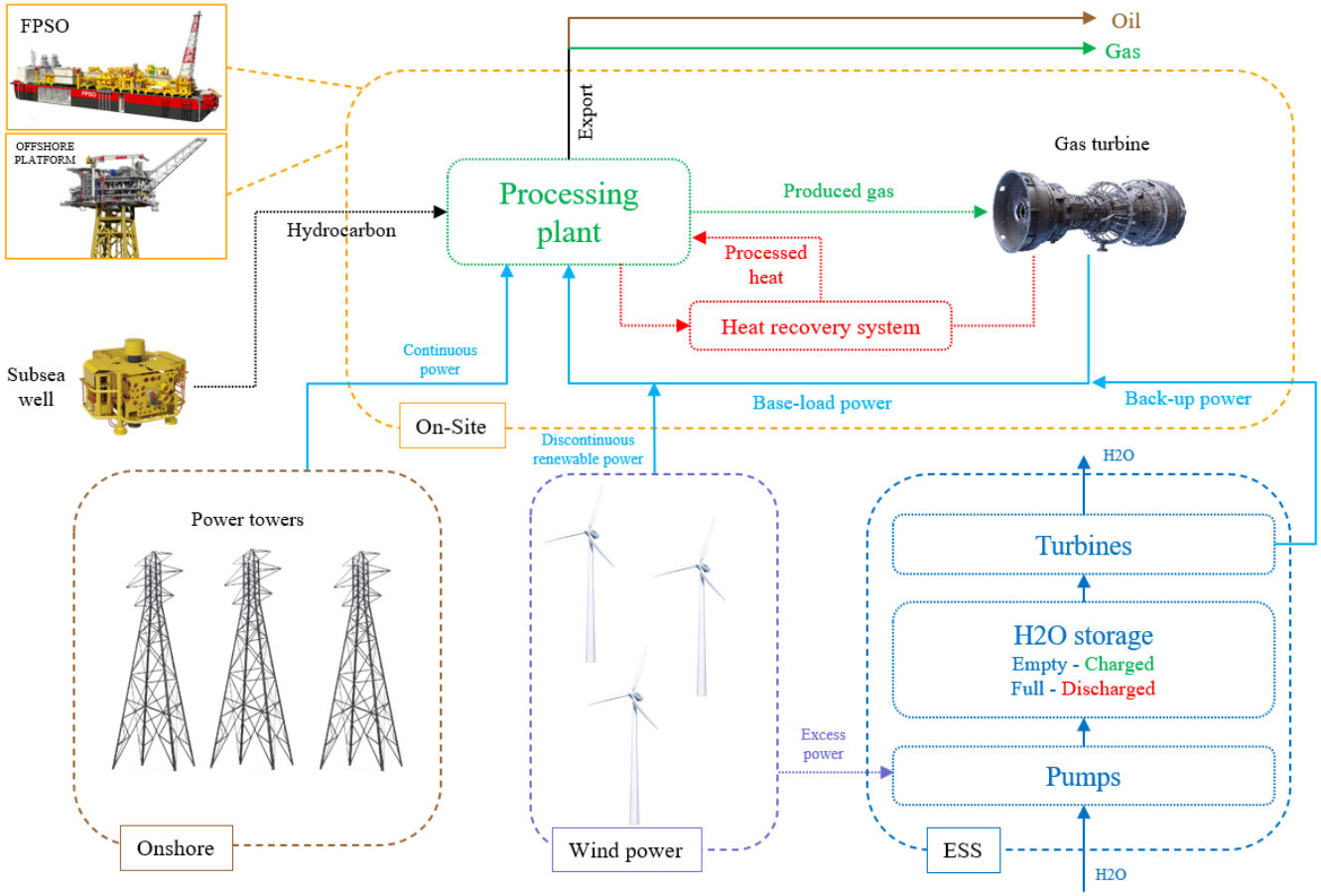

Figure 2 Schematic representation of the hybrid energy system using ESS.

This section describes the main power contributors that make up the hybrid energy system. The following process components meet the power demand of the offshore installation:

$$Load - P_{GT} + P_{WT} + P_{ESS} = 0 \quad (1)$$

where $Load$ is a power demand from the offshore platform, P_{GT} is gas turbine power output, P_{WT} is the wind power output, P_{ESS} is the power output from the ESS. All values are measured in megawatts (MW).

The power demand from the offshore platform and on-site facility is assumed to be constant throughout the whole operating period.

Gas turbines GE LM6000 PF with a rated power of 44.7 MW and GE LM2500 + G4 with a rated power of 33.3 MW examined by Riboldi [22] were chosen as the primary on-site power source. It is an aero-derivative gas turbines, usually used in offshore applications [6].

2.2 Wind power

The NREL offshore 5-MW baseline wind turbine was chosen as the primary source of wind power for this work [32]. The characteristics of the wind turbine are presented in Table 1:

Table 1 Properties of the NREL 5-MW wind turbine

Parameter	Value
Rating	5 MW
Rotor Orientation, Configuration	Upwind, 3 Blades
Control	Variable Speed, Collective Pitch
Drivetrain	High Speed, Multiple-Stage Gearbox
Rotor, Hub Diameter	126 m, 3 m
Hub Height	90 m
Cut-In, Rated, Cut-Out Wind Speed	3 m/s, 25 m/s
Cut-In, Rated Rotor Speed	6.9 rpm, 12.1 rpm
Rated Tip Speed	80 m/s
Overhang, Shaft Tilt, Precone	5 m, 5º, 2.5º
Rotor Mass	110,000 kg
Nacelle Mass	240,000 kg
Tower Mass	347,460 kg

Since proposed approaches for ESS charging estimation rely on the irregularity of wind power, it should be noted that this aspect is strongly connected with the wind and environmental conditions in the operated region.

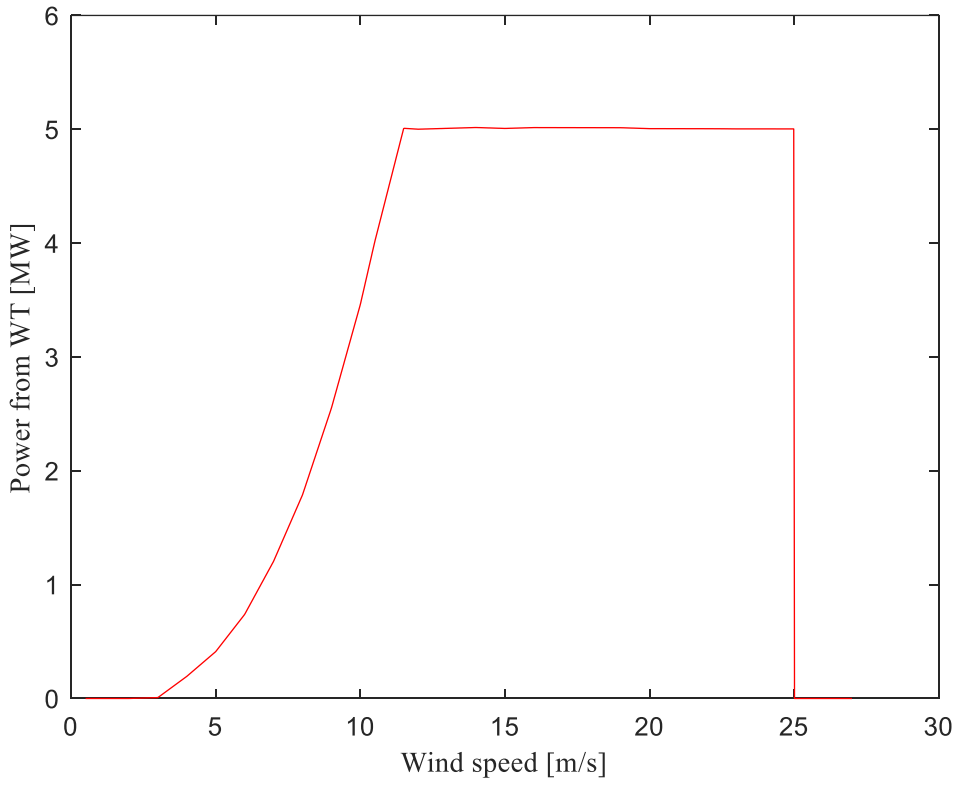

Figure 3 Wind turbine NREL 5 MW power output dependence on wind speed.

2.3 Energy storage devices

There are a variety of EES technologies available today. In this section, concepts that are currently being investigated are presented. Energy storage technologies applicable offshore and working in combination with wind power can be classified as follows:

Table 2 – Classification of the ESS technologies

Technology classification	Core technology	Working principle
Mechanical	CAES (Compressed Air Energy Storage) [47]	The storage is charged by the use of electrically driven compressors, which convert the electric energy into potential energy, or more precisely exergy, of pressurised air. The pressurised air is stored in CAS volumes of any kind and can then be released upon demand to generate electricity again by the expansion of the air through an air turbine
	Flywheels	
Electrochemical	Secondary Battery	Uses two electrodes and two different circulating electrolyte solutions, a positive and a negative, to convert and store electrical energy in the form of chemical energy and then convert that stored energy back into electrical energy
	Flow batteries [46]	
Electrical	SMES (Superconductor Magnetic Energy Storage) [45]	Stores energy in the magnetic field
	Supercapacitors	
Chemical (Hydrogen)	Power to Power (fuel cells, etc.) [22]	Hydrogen energy conversion system that converts the stored chemical energy in hydrogen to electrical energy, also producing water and heat as by-products with no carbon emissions
	Power to Gas	
Hydro	Subsea Energy Storage [23]	Generates electricity when water comes in and stores electricity when water is pumped out
	StEnSea (Stored Energy in the Sea) [35]	
	ORES (Ocean Renewable Energy Storage) [36]	
	Ocean Battery [37]	

Overview of the designs of the ESS technologies described in the Table 2 are presented on the Figure 4.

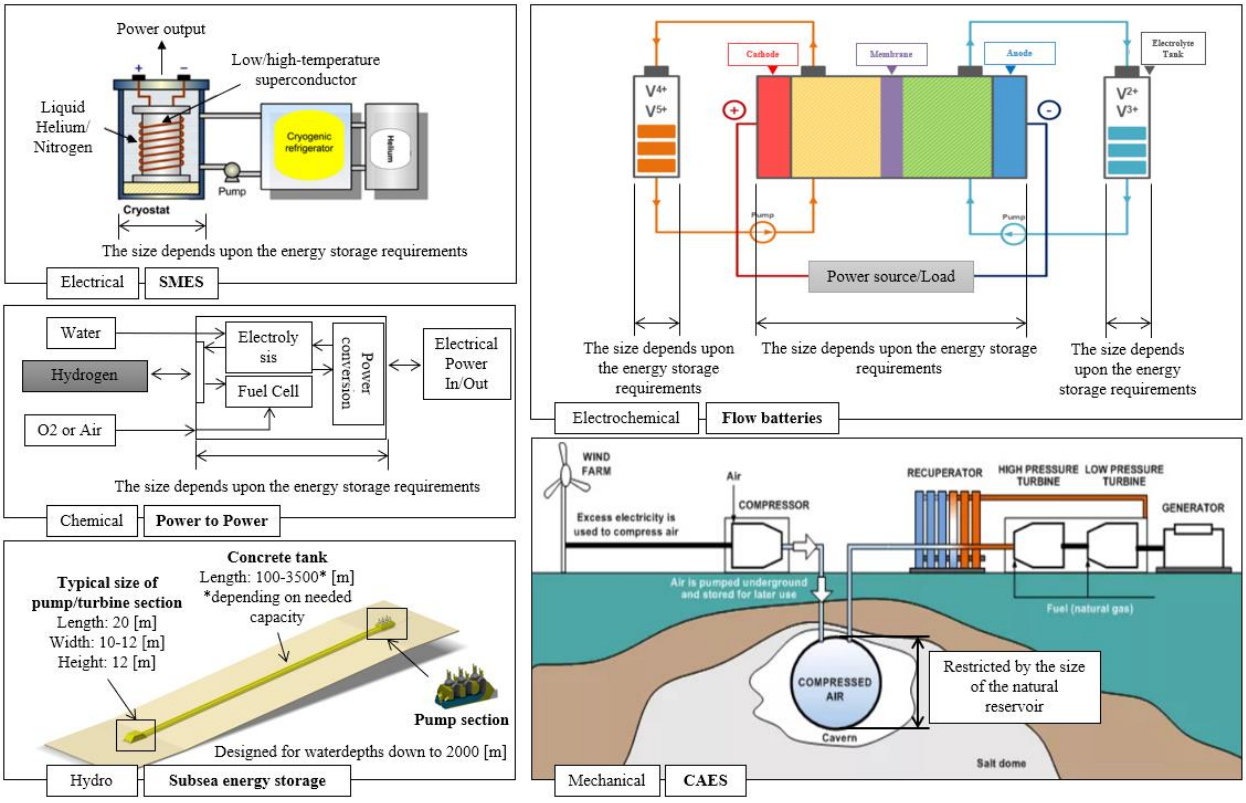

Figure 4 Overview of the energy storage designs.

3 Methodology

This part of the paper gives an overview of the methods used for sizing the energy storage system. Both methods analyse the wind data and wind distribution described in the section 3.1. Overview of methods 1 and 2 are presented in section 3.2 and 3.3 respectively. Verification of the methods through 50 years data is shown in the section 3.4.

3.1 Wind distribution

Wind speed distributions can be approximated well by the two-parameter Weibull distribution [40][41] and the probability density function (PDF) is given by Eq. 2.

$$f_{U_w}(u) = \frac{\alpha_U}{\beta_U}\left(\frac{u}{\beta_U}\right)^{\alpha_U - 1} * \exp\left[-\left(\frac{u}{\beta_U}\right)^{\alpha_U}\right] \quad (2)$$

where, α_U and β_U are the scale and shape parameters, respectively, and u is the wind speed variable, $f()$ refers to the PDF. It is shown in the Figure 5.

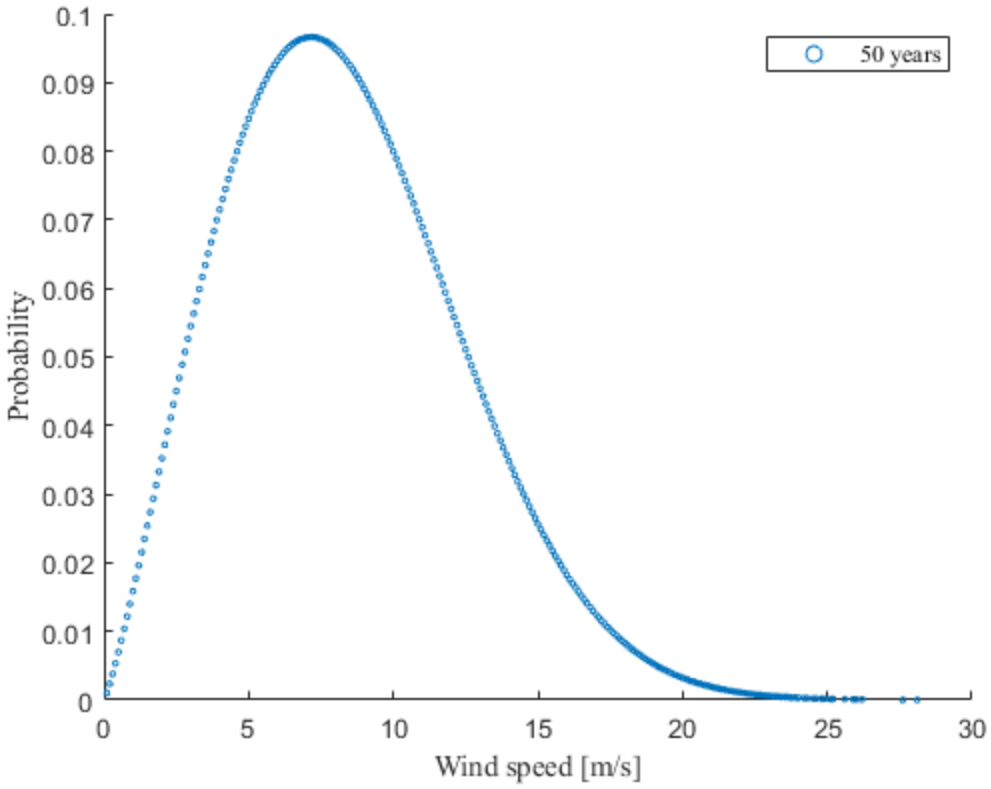

Figure 5 Weibull distribution for wind speed 50 years data in the Barents Sea

Since the data can be measured at different heights scaling parameter is needed to be used, which is represented by the equation 3 [33]:

$$U(z) = U_h * (\frac{z}{h})^{\alpha} \quad (3)$$

where z represents the height, U_h is the mean wind speed at the reference height h [m], $\alpha = 0.1$ - constant wind speed profile parameter.

3.2 Method 1: ESS sizing using expected wind speeds

This method refers to the sizing of an energy storage device considering wind power expected value. Since the wind speed varies during the time, there is different power contribution from the wind turbine in each time point. At the same time there is a value that occurs most often and can be obtained mathematically.

Firstly, the wind speed expected value is needed to be found. Using Weibull distribution from the Equation *2* shape parameter, β_U and scale parameter, α_U are obtained. These parameters are used to find wind speed expected value (Equation 4).

$$\overline{S_{wind}} = \alpha_U \, [\Gamma(1 + {\beta_U}^{-1})] \quad (4)$$

where, $\overline{S_{wind}}$ – wind speed expected value [m/s].

Secondly, using linear interpolation relying on the data from the Figure 3 wind power expected value is calculated (Equation 5).

$$\overline{P_{wind}} = P_{wind_t} + \frac{P_{wind_{t+1}} - P_{wind_t}}{S_{wind_{t+1}} - S_{wind_t}} (\overline{S_{wind}} - S_{wind_t}) \quad (5)$$

where, $\overline{P_{wind}}$ – wind power mean (expected) value [MW], t – data point, P_{wind_t} – wind power value in specific data point [MW], S_{wind_t} – wind speed value in specific data point [m/s].

Finally, ESS size is estimated solving simple equation 6.

$$\overline{P_{ESS}} = \overline{Load} - \overline{GT} - \overline{P_{wind}} \quad (6)$$

where, $\overline{Load}$ is mean installed demand from the offshore platform and facility, $\overline{GT}$ is mean power supply from the gas turbine. All values are measured in MW.

3.3 Method 2: ESS sizing using weather windows

The novelty of this work lies in the fact that to size the energy storage weather window analysis is used. Due to intermittent nature of wind, there are weather windows, where the value of the wind speed is such that the wind turbine cannot generate power. Maximum duration of the window is used to size ESS. Investigations are based on the 50 years wind data in the Barents Sea with 3-hour discretisation [42].

Firstly, depending on the type of the wind turbine (different hub heights, where extreme wind speed values are determined) equation 3 establishes wind speed boundaries, above and lower of which there is no power production (Figure 6**Error! Reference source not found.**).

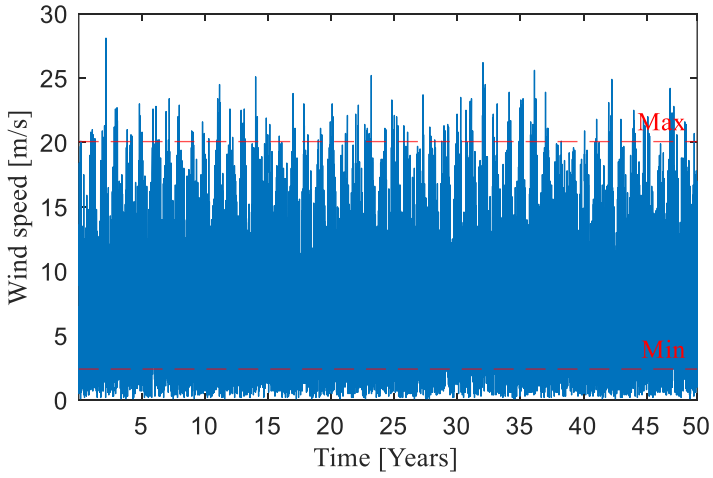

Figure 6 Wind speed boundaries within 50 years

Secondly, if there is a random sample of size N (wind speed 50-year data) from a distribution then we often estimate the cumulative distribution function (CDF) of that distribution by the empirical distribution function, which is just the number of observations divided by the total number N. In other words, the empirical distribution function is the distribution function of the discrete distribution, which puts probability 1/N on each of the observations. Using Equation 7 emperical CDF of the weather window durations is

obtained. It shows that below particular probability, the particular duration of the window is likely to occur [39].

$$Emperical\ CDF = \frac{i = 1, \dots, N}{N} \tag{7}$$

where, i – specific weather window, N – total number of weather windows without wind power output within 50 years.

Finally, according to the chosen cut-off (characteristic) value of the empirical CDF, which is equal from 0 to 1, value of non-productive hours (weather window duration) for which ESS should be designed is obtained. Estimation of the ESS size is done as follows:

$$E_{ESS} = \left(\overline{Load} - \overline{GT}\right) * h(p), p \in [0,1] \tag{8}$$

where, E_{ESS} – ESS charging [MW*h], h - weather window duration (non-productive hours) [h], p – cut-off (characteristic) value of empirical CDF.

3.4 Verification of methods 1 and 2 through 50 years data

A this stage, multiplication factor is introduced, which is empirically feeded to adjust the ESS design obtained in method 1 and method 2 to the minimum required size capable to operate within 50 years. (Equation 9).

$$\begin{aligned} 1\ method&: ESS_{50\ years} = \overline{P_{ESS}} * n \\ 2\ method&: ESS_{50\ years} = E_{ESS} * m \end{aligned} \tag{9}$$

where, n - number of hours ESS should be designed to be capable to sustain 50 years [h], m - multiplication factor.

4 Results and discussion

In this section, the results of the ESS sizing using method 1 and method 2 are discussed.

4.1 Base case

The Norwegian continental shelf was chosen as the study area. According to Legorburu [19], this area is considered extremely promising for the combination of offshore petroleum production facility and offshore wind farms when evaluating technical, environmental, and market aspects. There are 15 zones on the Norwegian shelf, including zones considered for bottom-fixed installations and floating turbines with a capacity factor is estimated to be in the range of 36–50% (from 4600 to 12600 MW), with an estimated average production of 19 – 60 TWh [19]. This assessment is supported by He [18], which describes that offshore wind displays higher average wind speed, lower turbulence intensity, and wind shear.

An offshore facility located in the Norwegian sector of the Barents Sea is used as a case study. The input data is presented in the Table 3.

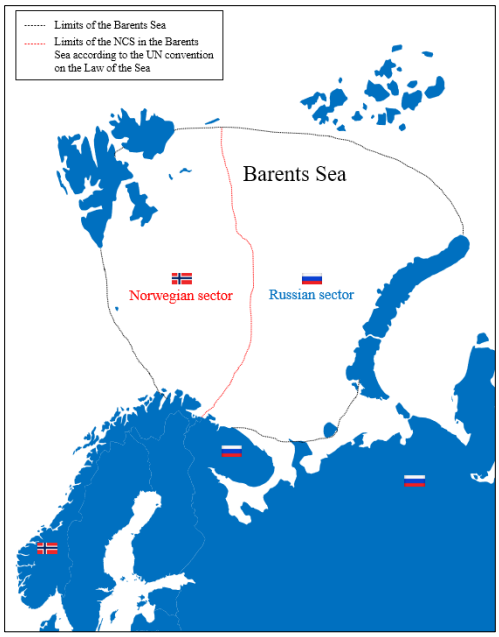

Figure 7 Norwegian and Russian sectors of the Barents Sea.

Table 3 – Input data

Parameter	Unit	Value
Load from the offshore platform and facility	MW	45.0
Gas turbine installed power output	MW	44.7
Gas turbine workload	-	0.95
Gas turbine operated power output	MW	42.5
Number of wind turbines	-	5
Initial state of charge of the ESS	%	50

The following aspects have been investigated:

- Size of the subsea energy storage;
- Comparison of the methods;
- Data sample influence on the results;
- Initial charging of the ESS;

4.1.1 Size of the storage required

Results of this work show that huge amount of power for ESS is needed to maintain constant power demand from the offshore facility. More than 500 MW*h of energy ESS should be capable to store for 50 years of operation (Table 4). Method 1 and 2 show comparable results varying from 2 – 10% depending on the wind power expected values, CDF curve and cut-off (characteristic) values used in the analysis.

Table 4 – Method 1, 2. ESS required charging for 50 years

Method	P^{*}_{ESS}, MW*h
Method 1	510
Method 2	

* - operated years = 50 years, assumed as work life of an offshore project

Charging of the ESS is not constant during the operation period. There are always surplus or deficit of power in the hybrid energy system due to wind power irregularity (Figure 8). Using the methods proposed in this paper helps to design ESS size capable to operate within different assumed time range and wind speed variations.

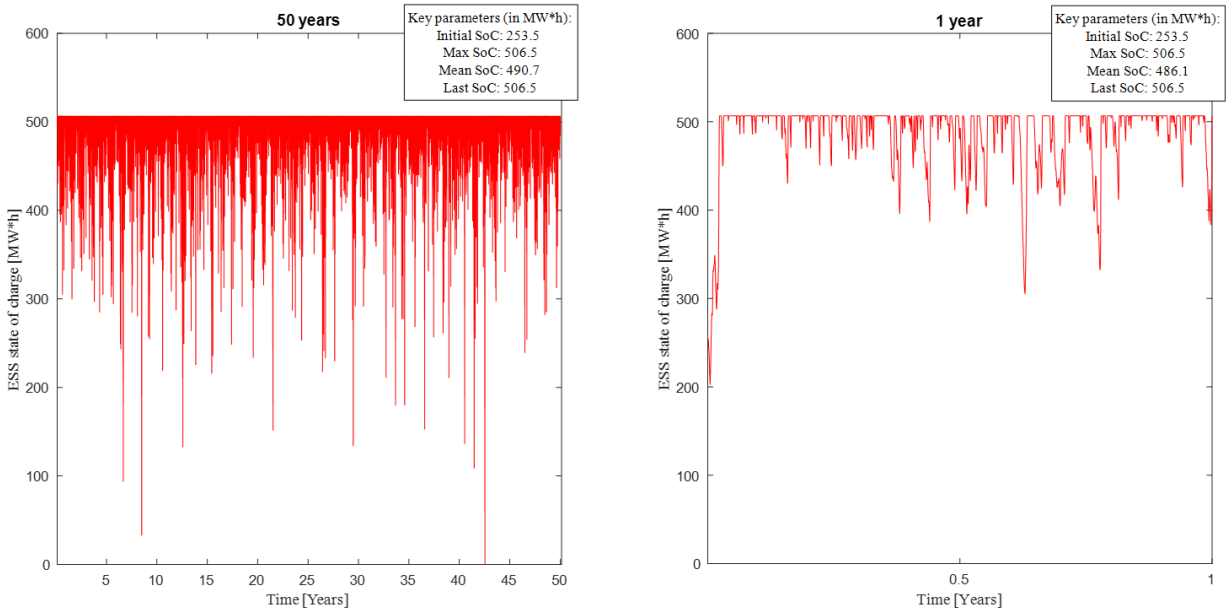

Figure 8 Method 1 - ESS state of charge over 50 years (left) and over 1 year (right) using wind power expected value for 50 years and 50% of initial charging

4.1.2 Method 1 vs. Method 2

Accuracy of methods

As it was mentioned in the section 4.1.1 method 1 and method 2 show comparable results, which are equal to the 510 MW*h on the average. Thus, both methods are applicable for the estimation of the ESS size and and comparable relative to each other. In terms of complexity, Method 1 is more intuitive and simpler to understand in comparison with the second method, where weather window analysis is used. Moreover, for Method 1 less wind data is needed, what is well-described in the next section.

Data sample size

Both methods clearly show that the large size ESS should be constructed for 50 years of operation. To obtain the values of the size multiplication factors were used. In the Method 1 multiplication factor is equal to the number of hours for which ESS should be designed. In the Method 2 this factor shows the value which should be applied to initially calculated ESS charging. It gives the result, which is equal to the ESS size capable to operate within 50 years.

Table 5 – Method 1. Base case. Results

Data sample*	$\overline{P_{wind}}$, MW	$\overline{P_{ESS}}$, MW	$n^{**}{}_{50\ yrs}$, hours
1 year	1.66	0.88	578***
15 years	2.02	0.52	976
25 years	2.03	0.51	998
50 years	2.07	0.46	1090

* - data sample in which wind power expected value is evaluated (return period)

** - mean energy storage capacity is tested in 50 years data

*** - multiplication factor - number of hours ESS should be designed to be capable to sustain 50 years

It is notable from the Table 5, that estimated data sample influences multiplication factor, since different expected values of wind speed and wind power are obtained. Starting from 5-year data sample these values are almost similar. This highlights the fact that using larger data sample more accurate results could be obtained.

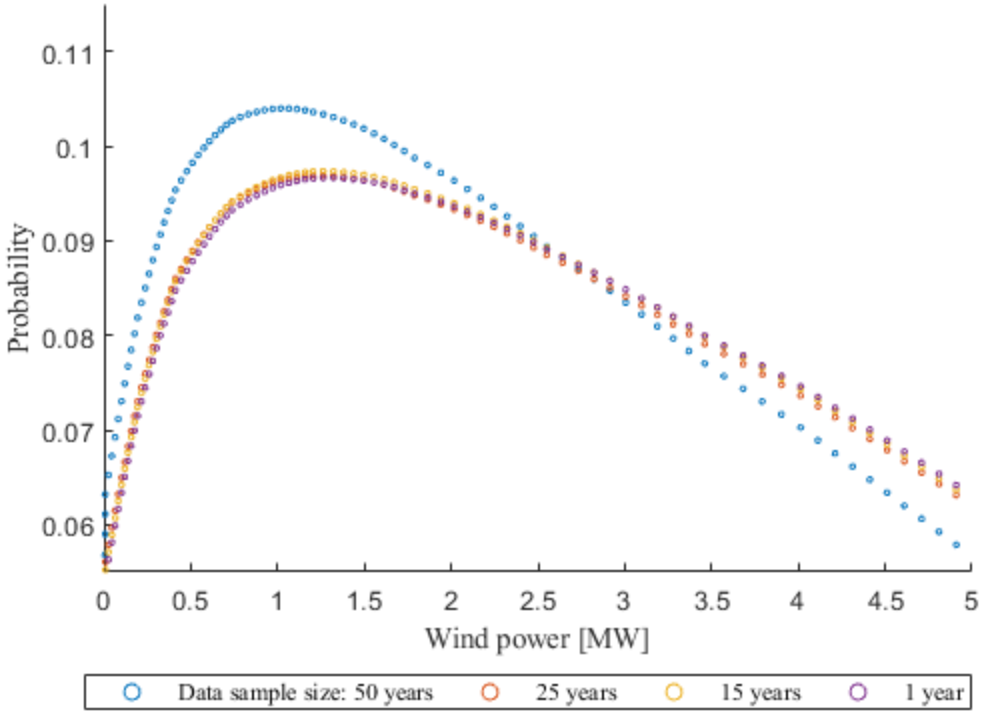

Figure 9 Probability of wind power supply for 50, 25, 15, 1 years

Table 6 shows, that multiplication factor relies on the chosen data sample as well as in Method 1. For 50 years of operation multiplication factor equaled to 76 will be enough to estimate the charging of ESS. Moreover, this factor is applicable for 15 and 25 years as well. Since the data sample of 1 year is relatively small to estimate the size, correspondingly, multiplication factor significantly differs compared to those where larger data samples are used. What is more, window duration depends on the cut-off value and, therefore, ESS charging value will be different depending on the chosen cut-off value (Figure 10).

Table 6 – Method 2. Base case. Results

Data sample*	Non-productive hours**	P_{ESS}, MW*h	$m^{***}_{50\ yrs}$
1 year	3.7	9.4	54
15 years	2.7	6.9	74
25 years	2.6	6.7	76
50 years	2.7	6.8	76

235 * - data sample used for CDF calculation

236 **- wind boundaries were scaled using Eq. 3, upper boundary at 10 m = 20.1 m/s, lower boundary at 10 m = 2.4 m/s

237 *** - multiplication factor using 50% cut-off value

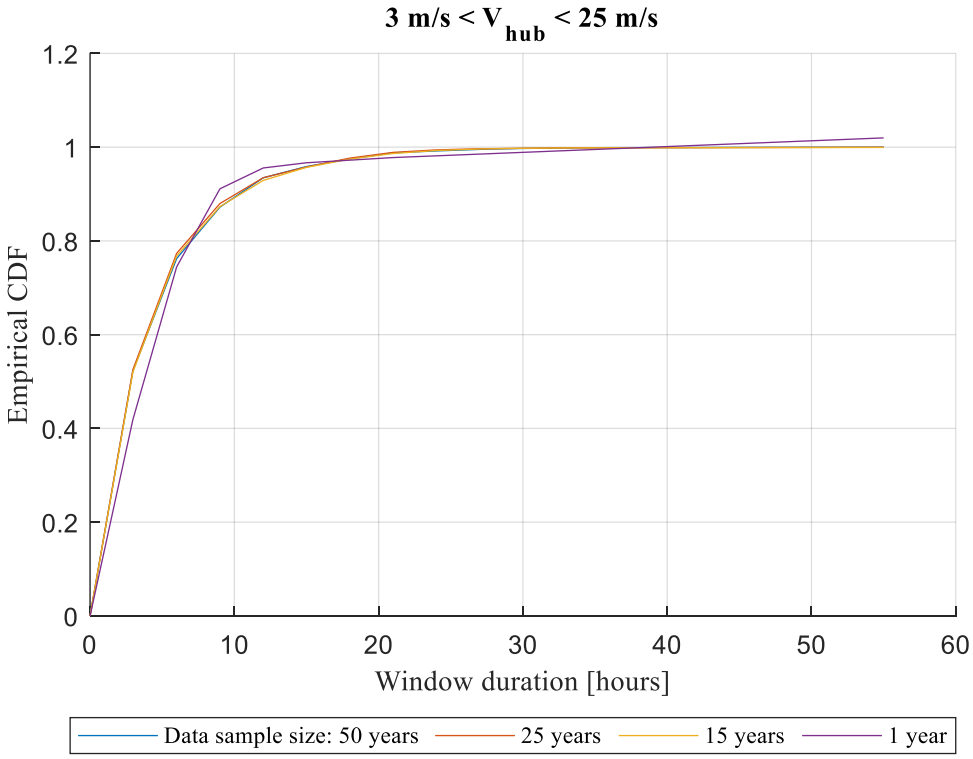

238

239 **Figure 10** CDF function for non-productive weather windows for 50, 25, 15, 1 years

240 Method 2 is found to be more sensitive to data sample size in comparison with Method 1. Standard deviation
241 of the results in Method 2 equals to 1.35, when in Method 1 this value equals to 0.09 (Table 7). Therefore,
242 the size of the data sample does not influence much the wind power expected value.

243 Sensitivity of the 2nd method to the data sample size is explained by the weather windows duration within
244 particular data sample and probability of its occurring. Larger data sample, more non-productive weather
245 windows fit into cumulative distribution function. From the other hand, variation of wind speed differs in
246 different data samples, which influences much the result and should be considered as well.

247

248

Table 7 – Data sample size influence on the ESS charging result

	P_{ESS}*, MW*h	
Data sample	**Method 1****	**Method 2*****
1 year	507.0	509.8
5 years	507.2	510.2
10 years	507.0	515.0
15 years	506.8	510.6
20 years	507.0	516.0
25 years	507.2	512.0
50 years	506.6	515.8

* - operated years = 50 years, assumed as work life of an offshore project

** - wind power expected value using different data samples

*** - CDF curve for different data samples using 50% cut-off value

Regarding influence of the data sample size on the multiplication factor for both methods it can be noticed from the Table 8 that accuracy of the result is strongly connected with the time period chosen as a data sample. For Method 1 the factor n should be equal at least 1000 to apply it to initially estimated ESS charging. This value can vary from 1-10% depending on the data sample used in the investigation, variation of wind speed within this data sample and obtained wind power expected value.

For Method 2 the magnitude of the factor m depends on the cut-off value used. It is noticeable from the Table 8 that 50% cut-off value requires application of the factor m equaled to 76, for 75% is 36 and 95% is 18, respectively. Thus, it is important to establish applicability of the multiplication factor for different cut-off values since it will affect the final result. These observations lead to the next point, where influence of the chosen cut-off value on the results is discussed.

Table 8 – Data sample size influence on the multiplication factor

	Multiplication factor*			
	Method 1	**Method 2**		
Data sample	n	$m_{50\%}$	$m_{75\%}$	$m_{95\%}$
1 year	578	54	34	18
5 years	984	70	34	14
10 years	886	72	36	14
15 years	976	74	36	16
20 years	958	74	36	14
25 years	998	76	36	16
50 years	1090	76	36	16

* - operated years = 50 years, assumed as work life of an offshore project

Cut-off (characteristic) value

According to the simulations provided for this paper, bigger cut-off values give bigger duration of non-productive weather windows. It means that the total number of these windows will be such that the storage will need to be designed with a larger size. It is shown in the Table 9. For cut-off values over 90% ESS initial charging should be about 560 - 580 MW*h. For the values equal and above 90% it is between 510 - 540 MW*h.

Table 9 – Comparison of the results for different cut-off values

Cut-off	$P^*_{ESS,50\ yrs}$, MW*h	$P_{ESS,25\ yrs}$, MW*h	$P_{ESS,15\ yrs}$, MW*h
95%	564.8	567.8	578.2
75%	533.4	521.4	527.6
55%	520.4	513.8	507.0
50%	515.8	512.0	510.6

Moreover, the survey shows that difference in the results for various data samples has the smallest deviation using 50% cut-off value, which gives expected values of non-productive weather window. It means that different data sample sizes and variations of wind speed give comparable values of the non-productive weather window duration on the average.

Table 10 – Standard deviation of the results for different cut-off values

Cut-off	Standard deviation, σ
95%	12.2
90%	4.1
75%	2.8
70%	3.1
55%	2.4
50%	**1.3***

* - for data samples from 1 to 50 years

4.1.3 Applicable multiplication factor

To sum up, the results for both methods show comparable values differing from 1-10% depending on the data sample size and cut-off value used for the estimation. The most applicable approach for Method 2 is using of the expected (mean) values of weather window duration or 50% cut-off value, which gives comparable results regardless of which data sample size and variation of wind speed are used. Since Method 1 using wind power expected value and data sample size does not influence much the result, mean value of the multiplication factor for data samples from 5 to 50 years can be used. Factors are presented in the Table 11.

Table 11 – Applicable multiplication factor for Method 1 and Method 2

Multiplication factor	
Method 1	**Method 2**
n	$m_{50\%}$
1000	76

4.2 Initial charging of the device

Charging of the device from the year 1 is another thing to consider. From the **Figure 8** charging of the ESS always faces the limits equaled to 510 MW*h if it is assumed to be 50% charged from the start. It means that there are time periods where excess power from the wind turbine is significant and can be stored in the storage device.

For the wind speed variation in the Barents Sea for 50 years ESS should be initially charged at least on 25% to be capable to sustain whole operation period or maintain all the fluctuation of wind power supply and not to be empty for 50 years. Initial SoC of 25% is equal to 130 MW*h. This value is a minimum from what ESS could start an operation, what is almost 5 times less compared to the 100% of initial SoC or 510 MW*h. During the operation period rest of the work will be done by wind turbines and excess power from it. For variation of SoC different multiplication factors are applied using Method 1 and Method 2 (Table 12). Proportionally, smaller value of initial SoC – smaller value of the multiplication factor is need. The main consideration here is manufacturing issues, which are quite challenging and needed to be discussed.

Table 12 – Multiplication factor depending on the initial charging of the device

	Multiplication factor	
Initial state of charge (SoC) of the ESS	**Method 1 - n^***	**Method 2 – $m^{**}_{50\%}$**
25 % - minimum	275	19
50 %	500	38
100 %	1100	75

* - wind expected value for 50 years

** - cut-off value = 50%

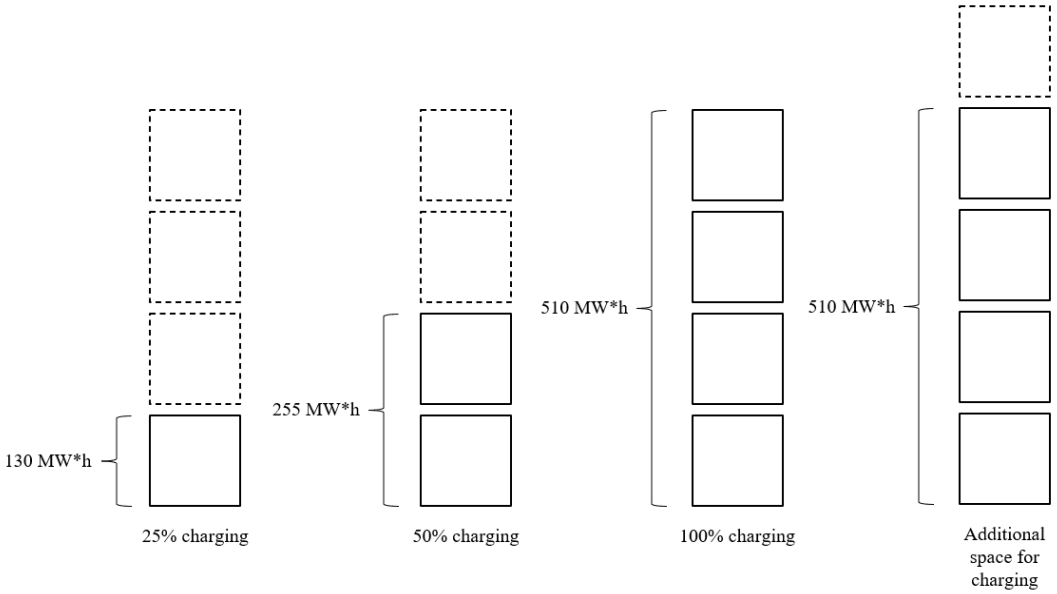

Figure 11 Options of device charging

Furthermore, it can be considered to size the device with an extra space for charging since there are always excess power which could be possibly stored. If the size of the storage will be increased by 2 times and will be equaled to the 1020 MW*h with the some characteristics as in the base case:

- Load from the platform: 45 MW;
- Gas turbine power output: 42.5 MW;
- Number of wind turbines: 5;
- Initial SoC: 255 MW*h;

It can be seen from the Table 13 that mean value of SoC will shift and will be equal 1003 MW*h. It says that according to the wind speed variation in the Barents Sea for 50 years, ESS can be designed with the size over 500 MW*h and can store over 1000 MW*h of energy. Such results obtained because 70% of time is surplus of power and only 30% is deficite which is distributed over 50 years. For more precise results and making classification which can be unique for the seas all over more offshore sites and wind speed variations are needed to be considered.

Table 13 – Mean SoC for different ESS size

Size of the ESS, MW*h	Mean SoC in 50 years, MW*h
510	499
1020	1003

What is more, in case of additional power demand and potential expansion of the offshore project larger size of ESS will be needed. It is a question of economic feasibility of this proposal. It can be costly to manufacture the ESS for the charging over 500 MW*h. Thus, precise calculation of the CAPEX and OPEX for long-term operation of the hybrid energy system should be made before manufacturing the energy storage device.

4.3 Additional power supply from the shore

Since in the base case ESS is needed to be large enough, the question arises about what alternative solutions of power grid design can be proposed to construct the ESS in smaller configuration with the saving of the concept with CO_2 emission decreasing and effective maintaining of power demand from the offshore facility.

To avoid the construction of large structures of subsea energy storage, contribution from the direct power source from the shore via subsea power cable can be considered as an alternative solution for the project on the continental shelf with a short step-outs (such as Laggan & Tormore [43], Corrib fields [44] and so on), where the power supply technologies from the shore is already tested and widely used. Results are shown in Table 15.

Alternative solution assumes modernisation of the base set-up with minimal losses of a power grid efficiency. Small size configuration of the gas turbine with rated power 33.3 MW was chosen [22]. Power from the shore is considered to be the cable connected to the already existed power plant onshore. Connecting to the power plant onshore will help to avoid additional expenses on the required facility for power production. All the aspects mentioned above will influence several factors:

- decrease of CO_2 emissions from the gas turbine;
- less expenses on the gas turbine;
- size decreasing of the ESS;
- reduction of the ESS manufacturing costs;
- reduction of the ESS installation costs;

Table 14 – Input data. Alternative case

Parameter	Unit	Value
Load from the offshore platform and facility	MW	45.0
Gas turbine operated power output	MW	33.3
Power from the shore	MW	9.6
Number of wind turbines	-	5
Initial state of charge of the ESS	%	50

Table 15 – Method 1,2. Sizing results. Alternative case

Method	P_{ESS}*, MW*h
Method 1 Method 2	360

* - operated years = 50 years, assumed as work life of an offshore project

It can be seen from the results, that the size of the ESS decreased almost on 30% compared to the base case, instead of 500 MW*h ESS size could be manufactured with the size equal to 360 MW*h. What is more, initial SoC is equal to 178 MW*h (50% initial SoC), which is approximately 70 MW*h less compared to the base case, where SoC was 255 MW*h. It means that power grid design can be adjusted in a way, when smaller type of the gas turbine is used, ESS could be designed in a smaller size configuration and HES can be connected to the already exploited technology of power supply from the shore.

5 Conclusion

This paper proposes a methodology for sizing subsea energy storage devices for offshore wind-powered oil and gas platforms. It consists of 2 methods. The first method is based on wind speed expected value estimation using Weibull distribution function. The second method relies on the weather window analysis considering weather windows without wind power contribution. The purpose of both methods is to estimate the ESS size capable to operate within 50 years in the hybrid energy system, consisting of the offshore platform with the processing plant, wind farm and gas turbine. As an alternative solution, power supply by the subsea power cable from the shore was proposed. The results show that subsea energy storage of huge size equled to 500 MW*h is required for 50 years of exploitation. Furthermore, both methods are applicable for sizing since they show comparable results. In addition, data sample size does not influence much the final sizing result and multiplication factor of method 1. This is mainly due to the fact that the mean wind speed in different time intervals is approximately the same. On the other hand, for method 2 sizing results differ by 2% due to different number of weather windows within particular data sample. What is more, the sizing result is affected by chosen cut-off (characteristic) value. Difference in the results can be 12% depending on the selected value. From the authors point of view more applicable is 50% cut-off value since it is the most common variant is within assumed time frame. Finally, it must be mentioned that initial state of charge of the device should be at least 25% to be cable to operate and the maximum size of the device could be expanded to more than 500 MW*h in the Barents Sea wind conditions. It is expected that this study can be used as a guide for planned and existing projects when it comes to sizing of the subsea energy storage.

Acknowledgment

The authors acknowledge the support from HK-dir UTFORSK Project (project number UTF-2017-four-year/10044) between University of Stavanger and Gubkin Russian State University of Oil and Gas.

References

[1] Our World in Data. (2022). *CO_2 and Greenhouse Gas Emissions*. https://ourworldindata.org/air-pollution

[2] Statistics Norway. (2021). *Emissions to air*. Statistisk Sentralbyrå. https://www.ssb.no/en/natur-og-miljo/forurensning-og-klima/statistikk/utslipp-til-luft

[3] DNV AS. (2021). *Energy transition Norway 2021 - A national forecast to 2050*. Retrieved from https://www.dnv.com/Publications/energy-transition-norway-2021-212201

[4] Norwegian government. (2019). *Regjeringa legg fram Noregs lågutsleppsstrategi for 2050*. Regjeringen. https://www.regjeringen.no/no/dokumentarkiv/regjeringen-solberg/aktuelt-regjeringen-solberg/kld/nyheter/2019-nyheter/regjeringa-legg-fram-noregs-lagutsleppsstrategi-for-2050/id2672248/

[5] KonKraft (2020). *The energy industry of tomorrow on the Norwegian continental shelf*. Retrieved from https://www.norskoljeoggass.no/contentassets/19ca8199a3b5459f850b1624ad0ee1c6/the-energy-industry-of-tomorrow-on-the-ncs----konkraft-report-2021-2.pdf

[6] Riboldi, L., Völler, S., Korpås, M., and Nord, L. O. (2019). An integrated assessment of the environmental and economic impact of offshore oil platform electrification. Energies 12, 2114. doi:10.3390/en12112114

[7] Nguyen, T.-V., Voldsund, M., Breuhaus, P., and Elmegaard, B. (2016). Energy efficiency measures for offshore oil and gas platforms. Energy 117, 325–340. doi:10.1016/j.energy.2016.03.061

[8] Roussanaly, S., Aasen, A., Anantharaman, R., Danielsen, B., Jakobsen, J., Heme-De-Lacotte, L., et al. (2019). Offshore power generation with carbon capture and storage to decarbonise mainland electricity and offshore oil and gas installations: a techno-economic analysis. Appl. Energy 233–234, 478–494. doi:10.1016/j.apenergy.2018.10.020

[9] Nguyen, T.-V., Barbosa, Y. M., da Silva, J. A. M., and de Oliveira Junior, S. (2019). A novel methodology for the design and optimisation of oil and gas offshore platforms. Energy 185, 158–175. doi:10.1016/j.energy.2019.06.164

[10] Norwegian Petroleum. (2022). *Emissions to air*. https://www.norskpetroleum.no/en/

[11] Zou, Xueqing, et al. "Sustainable offshore oil and gas fields development: Techno-economic feasibility analysis of wind–hydrogen–natural gas nexus." Energy Reports 7 (2021): 4470-4482. https://doi.org/10.1016/j.egyr.2021.07.035

[12] Hanssen, J. E., Margheritini, L., Mayorga, P., Hezari, R., O'Sullivan, K., Martinez, I., et al. (2015). "Design and performance validation of a hybrid offshore renewable energy platform," in Tenth International Conference on Ecological Vehicles and Renewable Energies (EVER), Monte-Carlo, Monaco.

[13] Korpås, M.; Warland, L.; He, W.; Tande, J.O.G. A case-study on offshore wind power supply to oil and gas rigs. Energy Procedia 2012, 24, 18–26. http://dx.doi.org/10.1016/j.egypro.2012.06.082

[14] Orlandini, V.; Pierobon, L.; Schløer, S.; De Pascale, A.; Haglind, F. Dynamic performance of a novel offshore power system integrated with a wind farm. Energy 2016, 109, 236–247. http://dx.doi.org/10.1016/j.energy.2016.04.073

[15] Riboldi, L.; Nord, L.O. Offshore Power Plants Integrating a Wind Farm: Design Optimisation and Techno-Economic Assessment Based on Surrogate Modelling. Processes 2018, 6, 249. http://dx.doi.org/10.3390/pr6120249

[16] Rafiee, A., and Khalilpour, K. R. (2019). Renewable hybridisation of oil and gas supply chains. Cambridge: Academic Press. 331–372. Book section 11. doi:10. 1016/b978-0-12-813306-4.00011-2

[17] NVE. (2013). Offshore wind power in Norway – Strategic environmental assessment. (NVE-rapport 47-12 Havvind). Retrieved from https://publikasjoner.nve.no/diverse/2013/havvindsummary2013.pdf
[18] He, W., Jacobsen, G., Anderson, T., Olsen, F., Hanson, T. D., Korpås, M., et al. (2010). The potential of integrating wind power with offshore oil and gas platforms. Wind Eng. 34, 125–137. doi:10.1260/0309-524X.34.2.125
[19] Legorburu, I., Johnson, K. R., and Kerr, S. A. (2018). Multi-use maritime platforms - North Sea oil and offshore wind: opportunity and risk. Ocean Coast Manag. 160, 75–85. doi:10.1016/j.ocecoaman.2018.03.044
[20] Aardal, A. R., Marvik, J. I., Svendsen, H., & Tande, J. O. G. (2012). Study of offshore wind as power supply to oil and gas platforms. In Offshore Technology Conference. OnePetro. https://doi.org/10.4043/23245-MS
[21] He, W., Uhlen, K., Hadiya, M., Chen, Z., Shi, G., & del Rio, E. (2013). Case study of integrating an offshore wind farm with offshore oil and gas platforms and with an onshore electrical grid. Journal of Renewable Energy, 2013. https://doi.org/10.1155/2013/607165
[22] Riboldi, L., Alves, E. F., Pilarczyk, M., Tedeschi, E., & Nord, L. O. (2020). Optimal design of a hybrid energy system for the supply of clean and stable energy to offshore installations. Frontiers in Energy Research, 8, 346. https://doi.org/10.3389/fenrg.2020.607284
[23] E. Kloster, S. Tonnessen, A. Akritidis, "Subsea energy storage," : US 2020/0347815 A1, 05.11.2020
[24] Riboldi, L., and Nord, L. O. (2017). Concepts for lifetime efficient supply of power and heat to offshore installations in the North Sea. Energy Convers. Manag. 148, 860–875. doi:10.1016/j.enconman.2017.06.048
[25] Kundur, P., Paserba, J., Ajjarapu, V., Andersson, G., Bose, A., Canizares, C., et al. (2004). Definition and classification of power system stability. IEEE Trans. Power Syst. 19, 1387–1401. doi:10.1109/TPWRS.2004.825981
[26] Fadaeinedjad, R., Moschopoulos, G., and Moallem, M. (2009). The impact of tower shadow, yaw error, and wind shears on power quality in a wind-diesel system. IEEE Trans. Energy Convers. 24, 102–111. doi:10.1109/TEC.2008. 2008941
[27] Honrubia-Escribano, A., Gómez-Lázaro, E., Molina-García, A., and Fuentes, J. (2012). Influence of voltage dips on industrial equipment: analysis and assessment. Int. J. Electr. Power Energy Syst. 41, 87–95. doi:10.1016/j.ijepes.2012.03.018
[28] Liang, X. (2017). Emerging power quality challenges due to integration of renewable energy sources. IEEE Trans. Ind. Appl. 53, 855–866. doi:10.1109/TIA.2016.2626253
[29] Alves, E., Sanchez, S., Brandao, D., and Tedeschi, E. (2019). Smart load management with energy storage for power quality enhancement in wind-powered oil and gas applications. Energies 12, 2985. doi:10.3390/en12152985
[30] Årdal, A. R., Undeland, T., and Sharifabadi, K. (2012). Voltage and frequency control in offshore wind turbines connected to isolated oil platform power systems. Energy Proc. 24, 229–236. doi:10.1016/j.egypro.2012.06.104
[31] Sanchez, S., Tedeschi, E., Silva, J., Jafar, M., and Marichalar, A. (2017). Smart load management of water injection systems in offshore oil and gas platforms integrating wind power. IET Renew. Power Gener. 11, 1153–1162. doi:10. 1049/iet-rpg.2016.0989
[32] Jonkman, J., Butterfield, S., Musial, W., & Scott, G. (2009). Definition of a 5-MW reference wind turbine for offshore system development (No. NREL/TP-500-38060). National Renewable Energy Lab.(NREL), Golden, CO (United States).
[33] Li, L., Gao, Z., & Moan, T. (2015). Joint distribution of environmental condition at five european offshore sites for design of combined wind and wave energy devices. Journal of Offshore Mechanics and Arctic Engineering, 137(3). doi.org/10.1115/1.4029842
[34] IEC (2015). Mobile and fixed offshore units - electrical installations (Geneva, Switzerland: International Electrotechnical Commission). Tech. Rep. IEC 61892:2015.
[35] Hahn, H., Hau, D., Dick, C., & Puchta, M. (2017). Techno-economic assessment of a subsea energy

storage technology for power balancing services. Energy, 133, 121-127. https://doi.org/10.1016/j.energy.2017.05.116

[36] Slocum, Alexander H., Gregory E. Fennell, Gökhan Dundar, et al. (2013). Ocean Renewable Energy Storage (ORES) System: Analysis of an Undersea Energy Storage Concept. Proceedings of the IEEE 101(4): 906–924. http://dx.doi.org/10.1109/JPROC.2013.2242411

[37] Hut, L. (2020). Investigating the structural behaviour of the Ocean Battery (Doctoral dissertation).

[38] Subsea 7 Official Web Page. (2022). *Technology*. https://www.subsea7.com/en/our-business/technology.html

[39] Li, L., Zhu, X., Parra, C., & Ong, M. C. (2021). Comparative study on two deployment methods for large subsea spools. Ocean Engineering, 233, 109202. https://doi.org/10.1016/j.oceaneng.2021.109202

[40] Bitner-Gregersen, E. M., and Haver, S., 1991, "Joint Environmental Model for Reliability Calculations," The First International Offshore and Polar Engineering Conference, Edinburgh, UK, pp. 246–253.

[41] Bitner-Gregersen, E. M., 2005, "Joint Probabilistic Description for Combined Seas," ASME Paper No. OMAE2005-67382.

[42] Reistad, M., Breivik, Ø., Haakenstad, H., Aarnes, O.J., Furevik, B.R., Bidlot, J.R., 2011. A high-resolution hindcast of wind and waves for the North Sea, the Norwegian Sea, and the Barents Sea. J. Geophys. Res.: Oceans 116 (C5).

[43] Upstreamonline. (2022). *More big impairments for Total in UK*. https://www.upstreamonline.com/online/more-big-impairments-for-total-in-uk/2-1-435618

[44] Alchetron (2022). *Corrib gas project.* https://alchetron.com/Corrib-gas-project#corrib-gas-project-f89b5572-a22e-4ee9-b304-bbd6b33289d-resize-750.jpeg

[45] L. Chen, Y. Liu, A. B. Arsoy, P. F. Ribeiro, M. Steurer and M. R. Iravani, "Detailed modeling of superconducting magnetic energy storage (SMES) system," in IEEE Transactions on Power Delivery, vol. 21, no. 2, pp. 699-710, April 2006, doi: 10.1109/TPWRD.2005.864075.

[46] Lundin, R., & Beitler-Dorch, B. (2018). Modelling and Analysis of Mobile Energy Transmission for Offshore Wind Power : An analysis of flow batteries as an energy transmission system for offshore wind power (Dissertation). Retrieved from http://urn.kb.se/resolve?urn=urn:nbn:se:mdh:diva-40082

[47] Marcus Budt, Daniel Wolf, Roland Span, Jinyue Yan. (2016). A review on compressed air energy storage: Basic principles, past milestones and recent developments, Applied Energy, Volume 170, Pages 250-268, ISSN 0306-2619, https://doi.org/10.1016/j.apenergy.2016.02.108.